Title page

Targeted manuscript:
Energy & Environmental Science

Title:
Ethanol production in syngas-fermenting *Clostridium ljungdahlii* is controlled by thermodynamics rather than by enzyme expression

Authors:
Hanno Richter[a,1], Bastian Molitor[a,1], Hua Wei[a], Wei Chen[b], Ludmilla Aristilde[a,2], Largus T. Angenent[a,2]

Author affiliations (Department, Institution, complete address):
[a] Department of Biological and Environmental Engineering, Cornell University, Riley-Robb Hall, Ithaca, NY 14853;
[b] Institute of Biotechnology, Cornell University, Ithaca, NY 14853
[1] These authors contributed equally to this work

Corresponding author information:
[2] Largus T. Angenent, Department of Biological and Environmental Engineering, 226 Riley-Robb Hall, Cornell University, Ithaca, NY 14853, Phone: 607-255-2480, Email: la249@cornell.edu;
Ludmilla Aristilde, Department of Biological and Environmental Engineering, 214 Riley-Robb Hall, Cornell University, Ithaca, NY 14853, Phone: 607-255-6845, Email: ludmilla@cornell.edu

Keywords:
Clostridium ljungdahlii; syngas fermentation; ethanol; solventogenesis; proteome; metabolome

Electronic Supplementary Information

Supplemental Material and Methods

Chemicals and Materials

Sequencing-grade acetonitrile (ACN), trifluoroacetic acid (TFA), and formic acid (FA) were purchased from Fisher Scientific (Fair Lawn, NJ). The iTRAQ kit and strong cation exchange (SCX) cartridges were purchased from AB Sciex (Foster City, CA). The Sep-Pak solid-phase extraction (SPE) cartridges were purchased from Waters (Milford, MA), and modified trypsin was purchased from Promega (Madison, WI). All other chemical reagents, unless otherwise noted, were obtained from Sigma Aldrich (Milwaukee, WI).

Bacterial strains and growth conditions

Clostridium ljungdahlii strain PETC, ATCC 55383 (ATCC, Manassas, VA) was cultured as previously described [1,2] at 35ºC in a two-stage syngas fermentation system with primarily acidogenic conditions (acetate formation) established in Stage A, and primarily solventogenic conditions (ethanol formation) in Stage B. Briefly, the system was composed of a Stage A continuously stirred tank reactor (CSTR) and a Stage B bubble column reactor (liquid volumes: 1L and 4L, respectively). An artificial syngas mixture (60% CO, 35% H_2, and 5% CO_2) was used as source of carbon, reducing equivalents, and energy. The gas was continuously fed to both bioreactor stages separately, and the gas flow rate was provided in excess of consumption. The two-stage system was continuously fed with modified *Clostridium carboxidivorans* P7

54 medium with 2-fold the concentration of minerals, trace elements and vitamins (2x
55 medium), without any yeast extract.[2] 2x medium was continuously fed at a rate of 40 mL
56 h^{-1} through Stage A into Stage B. In the reactor setup for the metabolome analysis,
57 Stage B was supplied with effluent from Stage A, plus additional fresh medium (40 mL
58 h^{-1}), amounting to 80 mL h^{-1} flow rate through Stage B.[2] Effluent from Stage B was
59 passed through a polyethersulfone hollow fiber cell recycle module (C22E-011-01N,
60 Spectrum Laboratories, Inc., Rancho Dominguez, CA) to remain high concentrations of
61 cells in Stage B. The OD_{600} typically fluctuated between 1-2 in Stage A, and reached
62 values of 10-20 in Stage B. The pH value was controlled at pH 5.5 in Stage A, and pH
63 4.5 in Stage B, using 2 M potassium hydroxide and 2 M hydrochloric acid.
64

65 **Routine analytical procedures**

66 Both fermentation stages were sampled daily, and cell density (OD_{600}), gas
67 consumption/production (CO, H_2, CO_2), and formation of fermentation products (acetic
68 acid, ethanol) were quantified *via* spectrophotometer, gas chromatography, and high-
69 performance liquid chromatography, respectively, as previously described.[3] Dry cell
70 weight (DCW) was calculated using a correlation-coefficient of 0.242 g DCW L^{-1} OD_{600}^{-1}.[3]
71 Culture purity was examined daily with a phase-contrast microscope.
72

73 **Proteome analysis**

74 **Cell harvest and protein extraction**

75 All steps for cell harvest and protein extraction were conducted at 4 ºC. *Cell harvest:*
76 After the fermentation system had reached stable acidogenic/solventogenic conditions

77 in Stage A/B, respectively, separate samples of Stage A (7.48 mL cell suspension at
78 OD_{600}=2.22) and Stage B (2.25 mL at OD_{600}=7.36), containing 4 mg DCW from each
79 stage, were taken and centrifuged. Each cell pellet was washed twice with 4 mL
80 Millipore water (15 Ohm/cm) before storing at -20ºC. *Protein extraction:* Cell pellets
81 were thawed on ice, resuspended in 4 mL of 2.5 mM phosphate buffer (pH 7.4),
82 homogenized by vortexing and lysed in a French Press at 8000 lb in^{-2}. Lysates were
83 centrifuged (4000g, 10 min), pellets were discarded, and each supernatant was
84 supplemented with 50 µL of 4 M urea and 5 µL of a 1% solution of
85 sodiumdodecylsulfate (SDS). Sample volume was reduced to ~200 µL in a Speed-vac
86 centrifuge (Eppendorf, Hauppauge, NY). Each sample was centrifuged again (12000g,
87 10 min), and the supernatants containing the proteins were kept for further analysis.
88 Protein concentration was determined with the Bicinchoninic acid assay (Micro BCA,
89 Thermo Fisher, Waltham, MA) as 5.03 and 3.75 mg/mL (Stage A and B sample,
90 respectively). Sample contaminants were 0.4 M urea, 0.02% SDS, and 1.5 mM
91 phosphate.

92 **Protein Digestion and iTRAQ Labeling**

93 While above work was conducted in the Angenent Lab, the following was performed
94 in the CORNELL Biotechnology resource center, Proteomics and Mass Spectrometry
95 Facility. Protein concentrations were verified by the Bradford assay using BSA as a
96 standard.[4]. Each sample was reconstituted in 0.2 M triethylammonium bicarbonate (pH
97 8.0). An aliquot (100 µg) of proteins in a total volume of 30 µl was denatured by adding
98 1 µl of 2% SDS and reduced with 2 µl of 50 mM Tris-(2-carboxyethyl)phosphine
99 (TCEP). Cysteine residues were blocked with 1 µl of 200 mM methyl

100 methanethiosulfonate (MMTS) using the iTRAQ Reagents kit (AB Sciex). The proteins
101 were then digested using an enzyme to substrate ratio of 1:10 sequencing-grade
102 trypsin (Promega) at 37°C overnight. The digested peptides were labeled with iTRAQ
103 reagents following the manufacturer's instructions (AB Sciex), using 114-tag and 115-
104 tag for peptides from acidogenic and solventogenic *Clostridium ljungdahlii* cells, while
105 116-tag (acidogenic) and 117-tag (solventogenic) were used for technical replicates.
106 Efficiency of iTRAQ labeling was assessed by 4000 QTRAP (AB Sciex). After labeling,
107 the four samples were combined and subjected to high pH reverse phase (hpRP)
108 fractionation.

109 **High pH Reverse Phase (hpRP) Fractionation**

110 The pooled iTRAQ labeled peptides were passed through SCX cartridges (AB
111 Sciex), then desalted by Sep-Pak SPE cartridges (Waters) for subsequent hpRP
112 separation. Fractionation by high pH reverse phase chromatography was performed as
113 described previously.[5] Briefly, the iTRAQ labeled tryptic peptides were reconstituted in
114 buffer A (an aqueous solution of 20 mM ammonium formate, pH 9.5) and loaded onto
115 an XTerra MS C18 column (Waters) with buffer A. The LC was performed with a
116 gradient from 10 to 45% of buffer B (80% ACN/20% 20 mM NH_4HCO_3 (aqueous)) in 30
117 min at a flow rate of 200 µl/min. Forty-eight fractions were collected at 1 min intervals
118 and pooled into a total of 12 fractions, based on UV absorbance at 214 nm and with a
119 multiple fraction concatenation strategy.[6] Collected fractions were then dried down in a
120 vacuum concentrator and reconstituted in 160 µl of 2% ACN/0.5% FA for nano LC-
121 MS/MS analysis.

122 **Nano LC-MS/MS Analysis by LTQ-Orbitrap Velos**

123 The samples were analyzed on a LTQ-Orbitrap Velos (Thermo-Fisher Scientific, San
124 Jose, CA) mass spectrometer with an UltiMate 3000 RSLC nano system (Thermo-
125 Dionex, Sunnyvale, CA) connected by “CorConneX” nano-ion source (CorSolutions
126 LLC, Ithaca, NY). “CorConneX” nano-ion source held an in house-packed nano column
127 with magic C18 (5 μm, 75 μm × 50cm, Bruker, Billerica, MA) connected to a 10 μm
128 analyte emitter (NewObjective, Woburn, MA). Each reconstituted fraction (5 μl) was
129 injected into a PepMap C18 trapping column (5 μm, 300 μm × 5 mm, Dionex,
130 Sunnyvale, CA) at a 20 μl/min flow rate for loading, and then separated on the in house-
131 packed nano column, using a 120 min gradient from 5 to 38% ACN in 0.1% FA at 300
132 nl/min, followed by a 5-min ramp to 95% ACN-0.1% FA and a 5-min hold at 95% ACN-
133 0.1% FA. The column was re-equilibrated with 2% ACN-0.1% FA for 20 min before the
134 next run. The instrument method for Orbitrap Velos was set up in data-dependent
135 acquisition (DDA) mode. In all experiments, after the survey scan acquired over a mass
136 range of *m*/*z* 375–1800 at a resolution of 30000, the 10 most intensive precursors were
137 selected for subsequent fragmentation using high energy collision dissociation (HCD)
138 with a resolution setting of 7500 for the mass range of *m*/*z* 100–2000. A threshold ion
139 count of 5000 was selected for fragmentation at normalized collision energy of 38%.
140 Dynamic exclusion parameters were set at repeat count 1 with a 20 s repeat duration,
141 an exclusion list size of 500, and 30 s exclusion duration with ±10 ppm exclusion mass
142 width. The activation time was 0.1 ms for HCD analysis. All data were acquired with
143 Xcalibur 2.1 software (Thermo-Fisher Scientific, Bremen, Germany). The nanospray
144 voltage was set at 1.5 kV in positive ion mode and the source temperature at 275°C.
145 The instrument was externally calibrated using Ultramark 1621 for the FT mass

146 analyzer. An internal calibration was performed using the background polysiloxane ion
147 signal at *m*/*z* 445.120025 as the calibrant.

148 **Protein Identification and Quantification**

149 Raw data files acquired from the Orbitrap Velos mass were converted into MGF files
150 using Proteome Discoverer version 1.3 (Thermo Fisher Scientific, Bremen, Germany).
151 Subsequent database searches were carried out by Mascot Daemon (version 2.3,
152 Matrix Science, Boston, MA) for both protein identifications and iTRAQ quantification
153 against the NCBI *C. ljungdahlii* Ref-sequence database. Trypsin was chosen as
154 cleavage specificity with a maximum number of two allowed missed cleavages.
155 Methylthiolation (Cys) and four-plex iTRAQ modifications on Lys and N-terminal amines
156 were set as a fixed modification, and oxidation (Met), deamidation (Gln, Asn), and 4-
157 plex iTRAQ on Tyr were used as variable modifications. The searches were performed
158 using a peptide tolerance of 10 ppm and a product ion tolerance of 0.1 Da. For further
159 filtering the decoy search option was enabled. The resulting data files were exported
160 and filtered for <1% false discovery rate at peptide level. Confident quantification of
161 each protein involved at least two unique peptides identified by Mascot with a complete
162 iTRAQ reporter ion series. Proteins identified within the same family were grouped in
163 Mascot protein family summary. The quantitative protein ratios were weighted and
164 normalized by the median ratio with outlier removal set automatic in Mascot for each set
165 of experiments. The manufacturer's recommended isotope correction factors were
166 applied. The functional annotation and classification of all proteins identified, and their
167 differential expression, were determined according to Blast2go (Bioinformatics
168 Department, CIPF, Valencia, Spain).[7] Protein abundances were calculated by the

169 emPAI method, which takes into account the number of sequenced peptides per
170 protein.[8]
171
172 **Metabolome analysis**
173 Levels of intracellular metabolites were determined in samples (three biological
174 replicates, each with three technical replicates), which were obtained from each reactor
175 stage (Stage A and Stage B). An aliquot (the volume was adjusted to contain 484 μg
176 DCW; *e.g.*, 2 mL sample volume at an OD_{600} of 1.0) of the cultures was filtered and the
177 metabolism was rapidly quenched by placing the filters in a 2 mL solution (4°C) of
178 methanol/ACN/water (40:40:20).[9,10] The supernatants with the released intracellular
179 metabolites were analyzed after the removal of lysed cell particulates *via* centrifugation.
180 Analysis was performed by reversed-phase ion-pairing liquid chromatography coupled
181 with electrospray ionization high-resolution mass spectrometry, which was operated in
182 full scan negative mode (*m/z* range 70–900), following established methods.[11]
183 Metabolite identification was based on accurate masses and validated by using
184 metabolite standards [10]. Metabolites were identified using the Metabolomics Analysis
185 and Visualization Engine (MAVEN) software package.[12] Metabolite levels were also
186 determined in cell-free samples, to account for accumulation of metabolites in the
187 fermentation broth, following removal of cells by centrifugation, and analyzed through
188 the same extraction procedure described above for the cell-rich sample before the LC-
189 MS measurements.[10]
190

Supplemental Results and Discussion

S1. Supplemental results for the metabolic schemes

S1.1 Metabolic schemes for growth on CO, H_2/CO_2, and fructose

Based on recent literature, we established metabolic schemes for growth of *C. ljungdahlii* with CO, H_2/CO_2, and fructose, to support conclusions drawn from our proteomics and metabolomics results. Our calculations are based on five considerations: 1) the energy-conserving role of the membrane-bound protein complexes, Rnf and ATPase has been elucidated[13,14], and ATP had been assumed to be generated in a stoichiometry of 1 mole of ATP/3.66 mole of protons (similar as in *Clostridium paradoxum*)[15]; 2) the production of reduced ferredoxin and NADPH by oxidation of H_2 *via* an electron-bifurcating hydrogenase was reported for *C. autoethanogenum*. The same hydrogenase directly reduces CO_2 (also when derived from CO oxidation) to formate in conjunction with formate dehydrogenase[15,16]; 3) the role of the electron-confurcating/-bifurcating Nfn complex has been discussed[15,17,18]; 4) the redox cofactors involved in redox reactions in the WLP have been experimentally addressed for *C. autoethanogenum*[15]; 5) the experimental proof is missing, but it is assumed that methylene tetrahydrofolate reductase (MetFV) is electron-bifurcating with ferredoxin and NADH.[15,19]

For fermentation of CO (**Figure S1a,b**), the net yield (mole ATP/mole product) can be determined as 1.503 ATP/acetate, 1.776-2.0492 ATP/ethanol (AOR route, depending on the cofactor specificity of ADHs), or 1.596 ATP/ethanol (ALDH route). These results suggest that alcohol production is beneficial for the ATP yield of *C. ljungdahlii*. However, if taking into account that 6 *vs.* 4 CO are consumed during ethanol *vs*. acetate

214 production, the energetic advantage of ethanol production disappears. Normalized per
215 mole substrate consumed, *C. ljungdahlii* should produce 0.376 ATP/CO when producing
216 acetate, 0.296-0.342 ATP/CO when producing ethanol *via* the AOR route, and 0.266
217 ATP/CO when producing ethanol *via* the ALDH route. For fermentation of H_2/CO_2
218 (**Figure S1c**), the net molar ATP yield is 0.956 ATP/acetate, 1.230 ATP/ethanol (AOR
219 route), or 0.776 ATP/ethanol (ALDH route). Normalized per mole substrate consumed,
220 the ATP yield per mol H_2 is lower than with CO: 0.239 ATP/H_2 when producing acetate,
221 0.205 ATP/H_2 when producing ethanol *via* the AOR route, and 0.129 ATP/H_2 when
222 producing ethanol *via* the ALDH route. For fermentation of fructose (**Figure S1d**), the
223 net ATP yield is 1.47 ATP/acetate, or 1.547 ATP/ethanol (ALDH route). Normalized per
224 mole substrate consumed, the net ATP yield per mole fructose is 4.410 ATP/fructose,
225 when producing acetate and 3.093 ATP/fructose, when producing ethanol. During
226 growth on H_2/CO_2 and hexoses for which less reduced ferredoxin is available per mole
227 of acetyl-CoA that is reduced to ethanol, the ALDH route seems to be more important,
228 since it does not utilize ferredoxin **(Figure S1, Table S1)**. Indeed, others had found with
229 gene disruption and complementation that the bifunctional (ADH/ALDH) AdhE2 enzyme
230 is of significant importance for ethanol production *via* the ALDH route during fructose
231 fermentation in *C. ljungdahlii.*[20] Importantly, CO_2 can be a byproduct of the fermentation.
232 When CO is the substrate, half of the carbon ends up in CO_2 when acetate is produced,
233 and two-thirds of the carbon ends up in CO_2 when ethanol is produced. When fructose
234 is the substrate, CO_2 from pyruvate oxidation can be recaptured *via* the WLP when
235 acetate is produced (homoacetogenesis), while one-third of the carbon ends up in CO_2
236 when ethanol is produced **(Table S1)**.

237 As mentioned above, CO gives higher ATP yields compared to H_2/CO_2. In agreement
238 with this, growth with CO can result in higher growth yields compared to H_2/CO_2.[21]
239 Higher ATP yields and more Gibbs free energy released during growth with CO *vs.*
240 H_2/CO_2 explain the improved growth rates and volumetric (ethanol) production rates.
241 Such improvements are only possible at CO concentrations that do not inhibit central
242 metabolism. It has been reported that high CO partial pressure can inhibit metabolism of
243 *C. ljungdahlii.*[22] This suggests that high CO partial pressure may not be a favorable
244 implementation for overcoming liquid-gas mass transfer limitations when designing
245 syngas fermentation systems. However, it has also been reported that high CO partial
246 pressures can be beneficial for ethanol production[23], and efficient co-fermentation of CO
247 and H_2 has been found in our two-stage bioreactor system.[1,2]
248

249 **S2. Supplemental results and discussion from the proteome analysis**

250 **S2.1 Ethanol production**

251 It has been known for several years that syngas-fermenting bacteria have the genetic
252 equipment to reduce acetate to acetaldehyde by an AOR enzyme *via* the indirect AOR
253 route (**Figure 1**).[19] Indeed, the mRNA of AOR genes was found to be abundant/up-
254 regulated during syngas fermentation in several studies.[24-26] More importantly, others
255 have proven the presence of an active AOR protein in *C. autoethanogenum* by
256 measuring the enzyme activity in cell extracts.[15] In addition, the AOR protein was found
257 in the proteome of *C. autoethanogenum* during syngas fermentation.[27] Here, we further
258 validated the importance of the indirect AOR route with our proteome data and found
259 that only this indirect AOR route is utilized to catalyze reduction of acetyl-CoA to ethanol
260 in *C. ljungdahlii* for our bioreactor conditions, rather than the direct ALDH route (**Figure**
261 **1**).

262 The **AOR route** involves the formation of acetate from acetyl-CoA *via* the Pta and
263 AckA enzymes. Acetate is then reduced to acetaldehyde by AOR (**Figure 1**). Four
264 potential AOR genes are present in the genome.[19] The proteins of three AOR genes
265 (CLJU_c20210, 15419 μmol/mol; CLJU_c20110, 13638 μmol/mol; and CLJU_c24130,
266 2542 μmol/mol) were found to be highly abundant (**Figure 1**). Others had already found
267 that the genes CLJU_c20210 and CLJU_c20110 were up-regulated on a mRNA level
268 during mid-exponential phase in *C. ljungdahlii* during fermentation of CO/CO_2.[24]
269 Meanwhile, CLJU_c24130 had been shown to be up-regulated on mRNA level upon
270 exposure to oxygen and might have a higher oxygen tolerance by utilizing molybdenum
271 instead of tungsten as cofactor.[28] The proteins of the other AOR gene (CLJU_c24050,

272 57 μmol/mol) were present at much lower levels in our proteome data. Thus, three out
273 of the four AOR proteins were highly abundant in our study even during acidogenesis.

274 The **ALDH route** involves direct reduction of acetyl-CoA to acetaldehyde with the key
275 enzyme ALDH. Three potential ALDH genes are present in the genome[19], but only one
276 corresponding protein was found in the proteome analysis (CLJU_c11960). This protein
277 was hardly detectable (11 μmol/mol), and therefore seems not important for ethanol
278 formation. However, since an alternative path within the ALDH route is possible without
279 using any of these three ALDH genes, we further analyzed this path that involves a
280 bifunctional ALDH/ADH (AdhE) enzyme to reduce acetyl-CoA into ethanol. Two proteins
281 (encoded by CLJU_c16510 [AdhE1] and CLJU_c16520 [AdhE2]) had previously been
282 found to be bifunctional ALDH/ADH enzymes.[19] But again, our proteomic data show that
283 these AdhE1 and AdhE2 proteins (each 6 μmol/mol) were not present at levels sufficient
284 to catalyze the high rates of ethanol production that we observed in our two-stage
285 bioreactor system during syngas fermentation **(Table S2)**. This is in agreement with
286 others, who found that mRNA levels of the *adhE1* and *adhE2* genes were significantly
287 down-regulated in *C. ljungdahlii* during autotrophic growth with CO or H_2/CO_2 *vs.*
288 heterotrophic growth with fructose.[25,26] Thus, the ALDH route was not found to be active
289 in our two-stage bioreactor system.

290 Without the ALDH route being important and with AOR proteins abundant, one or
291 more ADH protein(s) must be present to explain the reduction of acetaldehyde to
292 ethanol. In the genome, 19 potential ADH genes are present **(Figure 1)** {Köpke, 2010
293 #1390}. In our proteome data, only the CLJU_c39950 (55477 μmol/mol) protein was
294 highly abundant **(Figure 1, Table S3)**, thus, allowing ethanol formation after

295 acetaldehyde had been produced *via* the AOR route. This potential ADH protein, which
296 was initially described in the literature as a butanol dehydrogenase (BDH2) from
297 *C. ljungdahlii*, still showed about 70% activity toward ethanol in enzyme assays
298 (oxidation of alcohols to the corresponding aldehydes was measured).[29] The other
299 butanol dehydrogenase from the same study (BDH1, CLJU_c24880) with activity toward
300 ethanol was present in our proteomic data as well, albeit at a lower abundance (1082
301 μmol/mol). Our work is, therefore, in agreement with studies that found that the mRNA
302 levels for both BDH1 and BDH2 were up-regulated during syngas fermentation
303 compared to fructose fermentation.[25,26] In our proteome data without taking
304 CLJU_39950 into consideration, none of the ADH proteins were highly abundant (≥2500
305 μmol/mol, **Table S3**). However, some of the ADH proteins that were present at levels of
306 around 1000 μmol/mol may be also involved in ethanol production.

307 The second most abundant ADH protein, which is encoded by CLJU_c26570 (1513
308 μmol/mol), was originally annotated as a glycerol dehydrogenase. Its annotation does
309 not allow us to distinguish whether this enzyme participates in ethanol formation, or has
310 a different function. In addition, others have found a down-regulation on mRNA level of
311 CLJU_c26570 during fermentation of syngas *vs*. fructose.[25,26] Next, a primary-
312 secondary ADH had been characterized in *C. autoethanogenum* (CAETHG_0553).
313 CAETHG_0553 is homologous to CLJU_c24860 (248 μmol/mol, -1.7-fold), which,
314 therefore, might also have a different function than ethanol formation (*i.e.*, 2,3-
315 butanediol production).[30] Finally, the proteins CLJU_c23220 (903 μmol/mol, 2.0-fold),
316 CLJU_c18470 (829 μmol/mol, 4.9-fold), and CLJU_c23460 (678 μmol/mol, 1.4-fold),
317 which had not yet been characterized by others, are present in reasonable amounts and

318 might be involved in ethanol production, while the other candidate proteins are likely not
319 important for ethanol production under our conditions **(Figure 1)**.

320 Three of the most abundant ADHs (CLJU_c39950, CLJU_c24880, and
321 CLJU_c24860) had been shown to be NADPH-dependent.[29,30] The specificities for the
322 electron-donor of the other ADHs, also for the bifunctional AdhE enzymes, have not
323 been elucidated to our knowledge. It has been demonstrated that during growth on
324 fructose or H_2/CO_2 almost exclusively NADH-dependent ADH-activity was detectable in
325 cell extracts of *C. autoethanogenum.* During growth on CO, however, both NADH- and
326 NADPH-dependent ADH-activity was measured.[15] The presence of several
327 uncharacterized ADH-candidate enzymes found in reasonable amounts in our study
328 might explain both measured activities in the work by Mock *et al*.[15] The presence of
329 enzymes with different cofactor specificities may be beneficial when environmental
330 conditions change (in a similar way, as it may be beneficial that abundances of central
331 metabolic enzymes are not regulated).

332 In addition to our finding that the enzymes Pta and AckA are abundant during both
333 acidogenesis and solventogenesis, others had found that the mRNAs of the *pta* and the
334 *ackA* genes were up-regulated during late-exponential growth phase in *C. ljungdahlii*
335 during fermentation of CO/CO_2.[24] This finding further supports that the flux toward
336 acetate production and reduction to ethanol *via* acetaldehyde (AOR route) is not only of
337 great importance during acidogenesis, but also during solventogenesis.

338 **S2.2 Analysis of the proteome data**

339 Because we had found a close to equal distribution between the bioreactor stages
340 there did not seem to have been introduced a bias during sampling, processing, and

341 analysis. During solventogenesis, 78 proteins were up-regulated **(Table S4)** and 57
342 proteins were down-regulated **(Table S5)** more than 2.5-fold compared to acidogenesis.
343 But not all of these proteins were highly abundant because, by chance, only 3.5% (*i.e.*,
344 61/1743) of the proteins would be highly abundant (2-3 proteins; 3.5% from 57 down-
345 regulated proteins). The up-regulated proteins were over-represented in abundance,
346 though, since 12 out of the 78 up-regulated proteins were within the 61 highly abundant
347 proteins for the total proteome. With 2 out of the 58 down-regulated proteins being
348 highly abundant, this is as expected by chance **(Table S3-S5)**. There seems, thus, a
349 higher importance for the up-regulated than the down-regulated proteins for this
350 analysis.

351 **S2.3 Wood-Ljungdahl pathway**

352 Acetogenic bacteria use the WLP to fix carbon from CO_2 or CO into acetyl-CoA,
353 which is either further converted into biomass or utilized for energy conservation, under
354 concomitant production of mainly acetate and ethanol.[31] All relevant enzymes for this
355 pathway have been detected in our proteome analysis **(Figure 1)**.

356 **Hydrogenases.** We herein discuss six hydrogenases found in the genome of
357 *C. ljungdahlii*[2], although others have come to a different conclusion regarding the
358 number of hydrogenases.[19,32] One Ni/Fe-hydrogenase is encoded in the genome
359 (CLJU_c28660, 28670). The corresponding proteins were not detected here **(Figure 1)**.
360 However, several putative Ni/Fe-hydrogenase maturation proteins annotated to be
361 involved in the insertion of nickel (HypE1, HypD, HypF, and HypE2) were detected in
362 our proteome analysis (CLJU_c23060, 23070, 23090, and 36870).[33,34] Some of the
363 corresponding genes are clustered with nitrogenase genes. The corresponding proteins,

364 therefore, might have a different or an additional function than the insertion of nickel into
365 hydrogenases. Genes for three monomeric iron-only hydrogenases are present in the
366 genome (CLJU_c17280, 20290, and 37220). Two of the three corresponding proteins
367 were detected, although at very low levels, in our proteome analysis **(Figure 1)**.
368 Furthermore, two multi-subunit hydrogenases are encoded by the *C. ljungdahlii* genome
369 (CLJU_c14700-20, 07030-80). The first one (CLJU_c14700-20) is homologous to the
370 electron-bifurcating hydrogenase complex HydABCD, which depends on ferredoxin and
371 NAD^+, and is found in, for example, *Moorella thermoacetica* and *Acetobacterium*
372 *woodii*.[35,36] Only the CLJU_c14700 protein was detected in very low amounts **(Figure**
373 **1)**. The second multi-subunit hydrogenase (CLJU_c07030-80, HytA-E) is by far the
374 most abundant hydrogenase in our proteome analysis **(Figure 1)**. The homologous
375 enzymes in *C. autoethanogenum* bifurcate electrons from H_2 to $NADP^+$ and ferredoxin,
376 and form a complex with formate dehydrogenase (FDH) that functions as an enzyme
377 complex that directly reduces CO_2 to formate with H_2.[15,16] All relevant Hyt subunits were
378 present at high levels in *C. ljungdahlii* in our proteome analysis, and others had found
379 that the encoding genes are also highly transcribed/up-regulated on mRNA level under
380 autotrophic growth conditions compared to growth on fructose.[25,26] The abundance of
381 the CLJU_c07030-80 proteins (HytA-E) exceeded that of the other hydrogenases by
382 two orders of magnitude. Thus, this hydrogenase must be the primarily active
383 hydrogenase during syngas fermentation in *C. ljungdahlii*. Therefore, HytA-E is
384 responsible for the reversible reduction of $NADP^+$ and ferredoxin *via* electron-bifurcation
385 with H_2, as well as for the reduction of CO_2 to formate with H_2 in a complex with FDH
386 (see next paragraph; **Figure 1)**.

387 **Formate dehydrogenase (FDH).** Three different FDH proteins (encoded by
388 CLJU_c06990, 08930, and 20040) were detected in our proteome analysis, all of which
389 have homologous counterparts in *C. autoethanogenum.*[32] None of these three proteins
390 was differently abundant during acidogenesis and solventogenesis in *C. ljungdahlii*
391 **(Figure 1)**. This stands in contrast to observations made at mRNA level in
392 *C. autoethanogenum*.[37] There, mRNA expression of the CLJU_c06990 homolog ("FDH
393 seleno I") was down-regulated towards stationary phase, while expression levels of the
394 CLJU_c08930 homolog ("FDH non-seleno") and CLJU_c20040 homolog ("FDH seleno
395 II") were up-regulated toward stationary phase.[37] In another study, all three *fdh*
396 homologs were found to be up-regulated on mRNA level in the late exponential growth
397 phase.[24] These findings demonstrate that a change in mRNA expression levels during
398 stationary (non-growth) phase cannot necessarily be used to deduce a similar change in
399 protein levels and enzyme activities. The half-life of proteins (generally hours to days) is
400 much longer than that of mRNA (usually minutes).[38] This is especially relevant for the
401 stationary phase in which proteins are not diluted by cell division. Consequently, a
402 protein whose mRNA is down-regulated in stationary phase, can still be very abundant
403 and active, if it was produced during growth, and is not degraded by proteolysis.
404 Nevertheless, our proteomics data support the mRNA results because during
405 exponential growth the highest relative amount of *fdh* translate was found for
406 CLJU_c06990, which may, therefore, be the major functional FDH in *C. ljungdahlii*. This
407 finding is further supported by the genomic organization of CLJU_c06990, which is co-
408 located with genes coding for the HytA-E hydrogenase cluster discussed above. The
409 *fdh* gene and the *hytA-E* cluster are transcribed separately in *C. autoethanogenum*, but

410 the proteins form a functional enzyme complex that is responsible for the reduction of
411 CO_2 to formate.[15,16]

412 **Carbon monoxide dehydrogenase/acetyl-CoA synthase (CODH/ACS) complex.**
413 The CODH/ACS complex is encoded by CLJU_c37550, 37570, 37580, 37600 (ACS),
414 and CLJU_37660, 37670 (CODH), which are all located within the WLP gene cluster
415 and all proteins were found to be abundant during acidogenesis and solventogenesis in
416 our proteome analysis **(Figure 1)**. A second soluble CODH (CLJU_c09090-09110),
417 which is identified by Köpke *et al.*[19], was also abundant under both conditions **(Figure**
418 **1)**. It has been already discussed elsewhere that the main function of the CODH during
419 growth on H_2/CO_2 (and on fructose; **ESI** *Results and Discussion – metabolic scheme*
420 **S1.1**) is to catalyze the endergonic ferredoxin-dependent reduction of CO_2 to CO
421 (ferredoxin, E' ≈ -500 mV; CO, E° = -520 mV), while it mainly catalyzes the exergonic
422 reaction in the opposite direction during growth on CO.[15] It has been assumed that the
423 second CODH (CLJU_c09090-09110) is utilized by *C. ljungdahlii* for the exergonic
424 oxidation of CO to obtain reduced ferredoxin.[26] But since the respective mRNA is highly
425 up-regulated during growth on H_2/CO_2[26], and was found to be highly down-regulated
426 during growth on CO[25], it can be speculated that mainly the CODH/ACS complex
427 contributes to the oxidation of CO to CO_2, and that the function of the orphan CODH
428 might be to support the ferredoxin-dependent reduction of CO_2 during growth on
429 H_2/CO_2. It was already pointed out by Mock *et al.*[15], and is noteworthy here, that the two
430 existing CODHs in *Methanosarcina acetivorans* can be deleted separately without
431 affecting growth on CO, and therefore they most likely function in both directions *in*
432 *vivo*.[39,40] The aerobic-type CODH that was mentioned by Köpke *et al.*[19] (CLJU_c23590-

433 23610), was not detected in our proteome analysis, supporting their speculation that it is
434 not utilized in energy metabolism. One more gene is annotated as CODH
435 (CLJU_c17910), but the protein was also not detected.

436 **Formyltetrahydrofolate synthetase (CLJU_c37650, Fhs), bifunctional**
437 **methylenetetrahydrofolate dehydrogenase/formyltetrahydrofolate cyclohydrolase**
438 **(CLJU_c37630, FchA/FolD; additional orphan FchA, CLJU_c37640),**
439 **Methylenetetrahydrofolate reductase (CLJU_c37610, 37620, MetFV), and**
440 **Methyltransferase (CLJU_c37560, AcsE).** These other enzymes of the WLP were all
441 present at high levels during acidogenesis and solventogenesis **(Figure 1)**. It is
442 assumed that MetFV bifurcates electrons from 2 moles of NADH to reduce 1 mole of
443 methylenetetrahydrofolate (to methyltetrahydrofolate) and 1 mole of oxidized ferredoxin
444 (to reduced ferredoxin). Possibly, the enzyme forms a complex with EtfAB.[19] We also
445 used this assumption for our metabolic schemes **(ESI** *Results and Discussion –*
446 *metabolic scheme* **S1.1)**. However, the experimental proof for this is still missing.[15] The
447 genome of *C. ljungdahlii* contains five copies of the *etfAB* genes.[19] We could detect two
448 sets of proteins (EtfAB) and a single EtfA in our study (CLJU_c13880, EtfB, 45
449 µmol/mol; c13890, EtfA, 17 µmol/mol; c20330, EtfB, 231 µmol/mol; c20340, EtfA, 220
450 µmol/mol; c21580, EtfA, 29 µmol/mol), although at low levels. However, the enzymatic
451 outfit for this bifurcation reaction would be available, supporting the previous
452 assumption. Mock *et al.*[15] also discussed the possibility of another low-potential electron
453 acceptor with specific features that is different from the ferredoxin from *Clostridium*
454 *pasteurianum* used in their enzyme assays. Furthermore, from the three ferredoxins
455 encoded by CLJU_c01440, c01820, and c37530, we only found the last two in our study

456 (111 μmol/mol and 190 μmol/mol). We also found proteins for four putative thioredoxins
457 encoded in the genome (CLJU_c40500, 1059 μmol/mol; c27800, 350 μmol/mol) and the
458 corresponding thioredoxin reductases (CLJU_c40490, 870 μmol/mol; c27810, 64
459 μmol/mol), and several putative flavodoxins (CLJU_c14000, ND; c17600, 388 μmol/mol;
460 c19570, 33 μmol/mol; c24780, 267 μmol/mol; c34890, 242 μmol/mol). Thioredoxins
461 probably have other functions, such as redox regulation of protein function, and
462 signaling.[41] However, flavodoxins are known to replace ferredoxin under iron-limited
463 conditions, although at lower rates.[42] Interestingly, the putative flavodoxin protein
464 encoded by CLJU_c24780 is up-regulated (3.7-fold) during solventogenesis, suggesting
465 the possibility of iron limitation. However, the protein was not very abundant **(Table S4)**.

466 **S2.4 Energy metabolism and redox balance**

467 Oxidation of reduced substrates, such as CO, H_2, or hexoses, generates reduced
468 ferredoxin, NADPH, and NADH at specific ratios, depending on the involved pathways
469 and redox enzymes (**Figure S1, Table S1**).[15,18,43] From H_2 oxidation, electron-
470 bifurcating hydrogenase (HytA-E) likely generates reduced ferredoxin and NADPH at a
471 1:1 ratio.[15] The membrane-bound Rnf-complex is essential for energy conservation
472 during growth with H_2 and one-carbon compounds.[13,14,18,19,44,45] Rnf catalyzes the
473 electron transfer from reduced ferredoxin ($E' \approx -500$ mV) to NAD^+ ($E^{o\prime} = -320$ mV).
474 Thereby, it utilizes the Gibbs free energy released due to the difference of the redox
475 potentials, to pump one proton across the cell membrane per electron transferred, and
476 therefore a membrane potential is established.[3,18,45] The Rnf complex is also essential
477 for maintaining a sufficiently high cellular level of NADH. The proteins encoded by the
478 *rnf* genes (CLJU_c11360-11410) were abundant during acidogenesis and

479 solventogenesis, confirming their significance. Only the CLJU_c11400 protein
480 (annotated as RnfA, which is a trans-membrane subunit) was not detected in our
481 proteome analysis, which was not surprising, since the membrane proteome is in
482 principal not well covered in the utilized method.[46]

483 NADH-dependent reduced ferredoxin:$NADP^+$ oxidoreductase (Nfn) is an enzyme
484 involved in balancing cellular levels of redox cofactors. Nfn confurcates electrons, which
485 are derived from reduced ferredoxin and NADH, to reduce $NADP^+$.[17,18,45] Nfn is encoded
486 by CLJU_c37240, which is a homolog of CAETHG_1580 in *C. autoethanogenum*[32], and
487 was misannotated as glutamate synthase. Nfn is encoded by two separate genes (*nfnA*,
488 CKL_0459; *nfnB*, CKL_0460) in *C. kluyveri.*[17] Nfn has been reported to play an
489 important role for balancing the cellular concentrations of reduced ferredoxin, NADH,
490 and NADPH.[15] The CLJU_c37240 protein is abundant during acidogenesis and
491 solventogenesis **(Figure 1)**. When only hexoses are available as fermentation
492 substrates, NADH and reduced ferredoxin are produced at a 1:1 ratio *via* glycolysis and
493 pyruvate oxidation, with no primary source of NADPH. Therefore, the Nfn protein is
494 even more important under hexose-fermenting conditions, fulfilling a role analogous to
495 transhydrogenases in *E. coli* ensuring NADPH supply **(Figure S1d)**.[47] The importance
496 of the Nfn complex during growth on hexose sugars was recently confirmed in a study
497 comparing heterotrophic growth on fructose with autotrophic growth on syngas in
498 *C. autoethanogenum*.[27]

499 **S2.5 Stress-related proteins**

500 Some proteins related to stress responses were found to be highly abundant (≥ 2500
501 μmol/mol) during *both* acidogenesis and solventogenesis. The reverse rubrerythrin

502 CLJU_c39340 was highly abundant under both conditions (47230 μmol/mol, 1.1-fold)
503 **(Table S3).** CLJU_c39340 is homologous to the reverse rubrerythrin-1 and -2 from
504 *C. acetobutylicum*, which is involved in a general stress response, including exposure to
505 oxygen[48-50], and has been recently shown to participate in the response of *C. ljungdahlii*
506 upon oxygen exposure.[28] The predicted cold-shock protein CLJU_c33240 (predicted
507 CspA, 45746 μmol/mol, -1.2-fold) was the third most abundant protein in the cell **(Table**
508 **S3)**. Although, CspA is the major cold-shock protein in *Escherichia coli*, homologs have
509 been also shown to be involved in more general cellular processes, such as DNA
510 packaging and stress responses.[51] This indicated that *C. ljungdahlii* experienced
511 general stress conditions in both bioreactor stages. In addition, other proteins that are
512 known to be involved in a general stress response, such as protein protection by
513 chaperone systems, oxidative stress protection, regulation, signaling, and protein
514 digestion, were up-regulated during solventogenesis. For example, the abundant
515 chaperone system components GroEL (10439 μmol/mol) and GroES (1882 μmol/mol)
516 were up-regulated 3.7- and 3.8-fold, respectively **(Table S4)**. In addition, the heat-shock
517 proteins Hsp18a (164 μmol/mol) and Hsp18b (126 μmol/mol), which are also chaperone
518 systems, were both up-regulated 5.1-fold, albeit these proteins were not highly
519 abundant. Thus, *C. ljungdahlii* endured stress during both acidogenesis and
520 solventogenesis, with a slightly elevated stress response during solventogenesis.
521

522 **S3. Supplemental results and discussion on the metabolome analysis**

523 **S3.1 Results on the bioreactor run for the metabolome analysis**

524 For the metabolome analysis, we collected samples from a subsequent two-stage
525 bioreactor run. Samples for metabolomics need to be taken fresh and frozen samples
526 could not be utilized. The experimental run was performed with the identical setup, gas-
527 mixture, medium composition, and strain as before, resulting in very similar
528 performance conditions for Stage A **(Table S2)**. The bioreactor system had been
529 optimized with one change, though, because we had included a bypass of medium to
530 supply additional nutrients to Stage B. This led to a doubling of the flow rate and a
531 higher cell density (OD_{600} of 21.1 *vs*. 7.25) for the solventogenic Stage B bioreactor than
532 without the bypass, and therefore to a higher volumetric ethanol production rate and
533 ethanol concentration **(Table S2)**. However, the ethanol production rate when corrected
534 to the cell density of *C. ljungdahlli* culture was comparable **(Table S2)**, and nutrients
535 were still limiting the production rates rather than the gas/liquid mass-transfer rate of CO
536 and H_2. With an acetate and ethanol concentration of 60.74 mM and 428.6 mM,
537 respectively, the ethanol-to-acetate ratio was 7.15 for Stage B **(Table S2)**, which was
538 comparable to the experimental run without the bypass (5.69).

539 **S3.2 Discussion on blank measurements for the metabolome analysis**

540 With the metabolome analysis, the intention was to measure intracellular levels of
541 metabolites in central metabolic pathways (**Figure 2, Table S7,S8**). However, the
542 challenge with obtaining intracellular metabolite levels in filtered cells from long-term
543 bioreactor runs is the interference of accumulated metabolites in the extracellular milieu
544 from: 1) excretion of metabolites by viable cells; and 2) release of metabolites by lysed

545 cells.[52] These extracellular metabolites can interfere due to the retention to filter
546 materials during processing of the cell-rich samples. To account for such interference,
547 we conducted a blank measurement of cell-free extracellular metabolites, but we did not
548 correct for the intracellular metabolite levels by subtraction (**ESI** *Material and Methods*).
549 Instead, we calculated whether the comparison between the cell-rich samples from
550 acidogenesis and solventogenesis was statistically significant only when the criteria of a
551 sample-to-blank ratio of 10:1 had been met for both conditions **(Table S7)**.
552

553 **S4. Supplemental results for the overflow model**

554 **S4.1 Effects of extracellular pH and total acetate concentration**

555 Undissociated acetic acid can freely diffuse into the cell. Therefore, the intracellular
556 total acetate concentration depends on the extracellular pH, resulting in higher
557 intracellular total acetate concentrations at lower external pH values. This, because
558 after diffusion of undissociated acetic acid into the cell, the acetic acid will dissociate to
559 acetate at an assumed intracellular pH of 6[15], where only ~5% of the total acetate is in
560 the undissociated acetic acid form (pKa of acetate/acetic acid is 4.8). Active transport
561 (export) of acetate may lower the total intracellular acetate concentration again. With
562 only 5% undissociated acetic acid, the intracellular concentration of acetic acid will not
563 change drastically by increasing the extracellular acetic acid concentration or by
564 lowering the extracellular pH. However, the intracellular total acetate concentration will
565 increase at high extracellular undissociated acetic acid concentrations due to diffusion
566 and dissociation. As mentioned in the main text, the undissociated acetic acid is the
567 substrate for ethanol production. On the other hand, dissociated acetate is the main
568 product of the acetate production pathway from acetyl-CoA (Pta and AckA reactions).
569 Since the total acetate and the dissociated acetate (~95% at an assumed intracellular
570 pH of 6) are very dependent on the total acetate concentration and the extracellular pH,
571 the thermodynamic feasibility of the acetate production pathway is affected
572 considerably. A higher dissociated acetate concentration could make the acetate
573 production pathway thermodynamically unfeasible. Indeed, in our bioreactor study, we
574 found ethanol production already at an external pH of 5.5 in Stage B. When we lowered
575 the pH to 4.5 the ethanol production rate (normalized to cell density) remained constant,

576 while the acetate production rate (normalized to cell density) considerably decreased.[2]
577 From this follows, that we had reached an intracellular acetic acid concentration
578 permissive for ethanol production already at pH 5.5 in the Stage B bioreactor due to
579 nutrient limitations (without lowering the pH). However, we were able to increase the
580 ethanol-to-acetate ratio by lowering the extracellular pH to 4.5. This occurred due to a
581 higher undissociated acetic acid concentration in the extracellular milieu, resulting in
582 diffusion into the cell, dissociation at an assumed intracellular pH of 6, and a higher
583 dissociated acetate concentration, which makes the acetate production pathway less
584 feasible.

585 **S4.2 Discussion on our model for a single-stage bioreactor system**

586 When growth is fast with a high supply of nutrients, the relatively low ATP yield can
587 still limit biomass production yields in syngas fermentation. The bacterium would then
588 not be capable in re-oxidizing all reducing equivalents. Our model predicts that this
589 scenario would lead to ethanol production during growth. Indeed, by supplying
590 *C. autoethanogenum* with surplus nutrients and a constant supply of gas (H_2/CO_2) in a
591 one-stage CSTR bioreactor, a molar ethanol-to-acetate ratio of ~1:1 was achieved
592 during growth.[15] Furthermore, Mock *et al*. found that during fermentation of the more
593 reduced substrate CO (compared to H_2/CO_2) under these non-growth limited conditions,
594 *C. autoethanogenum* produced ethanol, acetate, and 2,3-butanediol in a 2:1:1 molar
595 ratio.[15] We did not find the enzymes for 2,3-butanediol production – acetolactate
596 synthase (CLJU_c38920, 4 µmol/mol), acetolactate decarboxylase (CLJU_c08380, 23
597 µmol/mol), and 2,3-butanediol dehydrogenase (CLJU_c24860, 248 mol µmol/mol) – to
598 be abundant in our proteome analysis with *C. ljungdahlii*. Therefore, we did not include

599 2,3-butanediol in our study because the HPLC peaks remained very small. However,
600 the model can be extended with 2,3-butanediol as a next overflow product when growth
601 nutrients are present, albeit more research would be necessary to test the universality
602 between different syngas-fermenting bacteria.
603

604 # Supplemental Figure Legends

605 **Figure S1.** Metabolic schemes for growth of *C. ljungdahlii* with CO **(a,b)**, H_2/CO_2 **(c)**,
606 and fructose **(d)**. Reactions are shown in the relevant direction with stoichiometries (in
607 moles) for substrates, products, reducing equivalents (NAD(P)H, ferredoxin), and ATP.
608 **(a)** Growth on CO (assuming NADH-specificity for ADH). Numbers in red are for
609 acidogenesis and numbers in brackets are for solventogenesis (light blue, AOR route
610 with NADH-specific ADH; dark blue, ALDH route). When only one number is given (in
611 brackets), the stoichiometry for acetate and ethanol production (or both "solventogenic"
612 routes) is the same. **(b)** Growth on CO (assuming different electron donor-specificities
613 for ADH). Only solventogenesis *via* the AOR route is shown. Light blue numbers are
614 assuming NADPH-dependent ADH activity, while dark blue numbers assume both
615 NADH- and NADPH-dependent ADH activity at a 1:1 ratio. When only one number is
616 given the stoichiometry for both scenarios is the same. **(c)** Growth on H_2/CO_2. Numbers
617 in red are for acidogenesis and numbers in brackets are for solventogenesis (light blue,
618 AOR route, only NADH-dependent ADH activity; dark blue, ALDH route). When only
619 one number is given (in brackets), the stoichiometry for acetate and ethanol production
620 (or both "solventogenic" routes) is the same. **(d)** Growth on fructose. Numbers in red are
621 for acidogenesis and numbers in dark blue are for solventogenesis (ALDH route, only
622 NADH-dependent ADH activity). When only one number is given, the stoichiometry for
623 acetate and ethanol production is the same. CO_2 produced during oxidative
624 decarboxylation of pyruvate is fixated through the WLP only during acidogenesis (purple
625 boxes). ATP is highlighted in bright red. Grayed out reactions are not relevant for the
626 particular growth conditions but might become active on different substrates. Acetyl-P,

627 acetyl-phosphate; CoFeS-P, corrinoid iron-sulfur protein; Nfn, NADH-dependent
628 reduced ferredoxin:$NADP^+$ oxidoreductase; Rnf, (membrane-associated) reduced
629 ferredoxin:NAD^+ oxidoreductase; THF, tetrahyfrofolate.
630
631 **Figure S2.** Performance of the two-stage fermentation system during continuous
632 operation for 1850 h (77 days) from which we sampled for proteome analysis. Data for
633 **(a)** growth (OD_{600}) and pH; **(b)** concentration of the fermentation products acetate and
634 ethanol in mM; **(c)** the average daily rates of consumption (negative) and production
635 (positive) in mmol min^{-1} for CO, H_2, and CO_2; **(d)** the average total daily feed rate of
636 medium in mL h^{-1}. The arrow and the dotted line indicate the day of sampling for the
637 proteome analysis. After 1488 h of operation Stage A was bypassed completely and run
638 as batch and Stage B was run as a single stage continuous reactor with a feed rate of
639 80 mL h^{-1}.
640
641 **Figure S3.** Overview of all measured metabolites in three biological replicates (B1, B2,
642 and B3). Error bars indicate technical replicates (*n=3*). Intracellular metabolite levels
643 and blank measurements (**ESI** *Materials and Methods*) obtained for the two different
644 growth conditions (acidogenesis, A; red, sample; light red, blank; solventogenesis, S;
645 blue, sample; light blue, blank) are shown. Values for all metabolites are given in **Table**
646 **S7 and S8**. Ac-P, acetyl-phosphate; Cit, citrate; Isocit, isocitrate; 2-KG, 2-ketoglutarate;
647 Pyr, pyruvate; PEP, phosphoenolpyruvate; OA, oxaloacetate; Mal, malate; Fum,
648 fumarate; Suc, succinate; 2-P-G, 2-phosphoglycerate; 3-P-G, 3-phosphoglycerate; 1,3-
649 BPG, 1,3-bisphosphoglycerate; GAP, glyceraldehyde 3-phosphate; DHAP,

650 dihydroxyacetone phosphate; F-1,6-BP, fructose-1,6-bisphosphate; Sedo-7-P,
651 sedoheptulose-7-phosphate; Ery-4-P, erythrose-4-phosphate; F-6-P, fructose-6-
652 phosphate; G-6-P, glucose-6-phosphate; Xyl-5-P, xyloulose-5-phosphate; R-5-P,
653 ribulose-5-phosphate.

Supplemental Figures

Figure S1

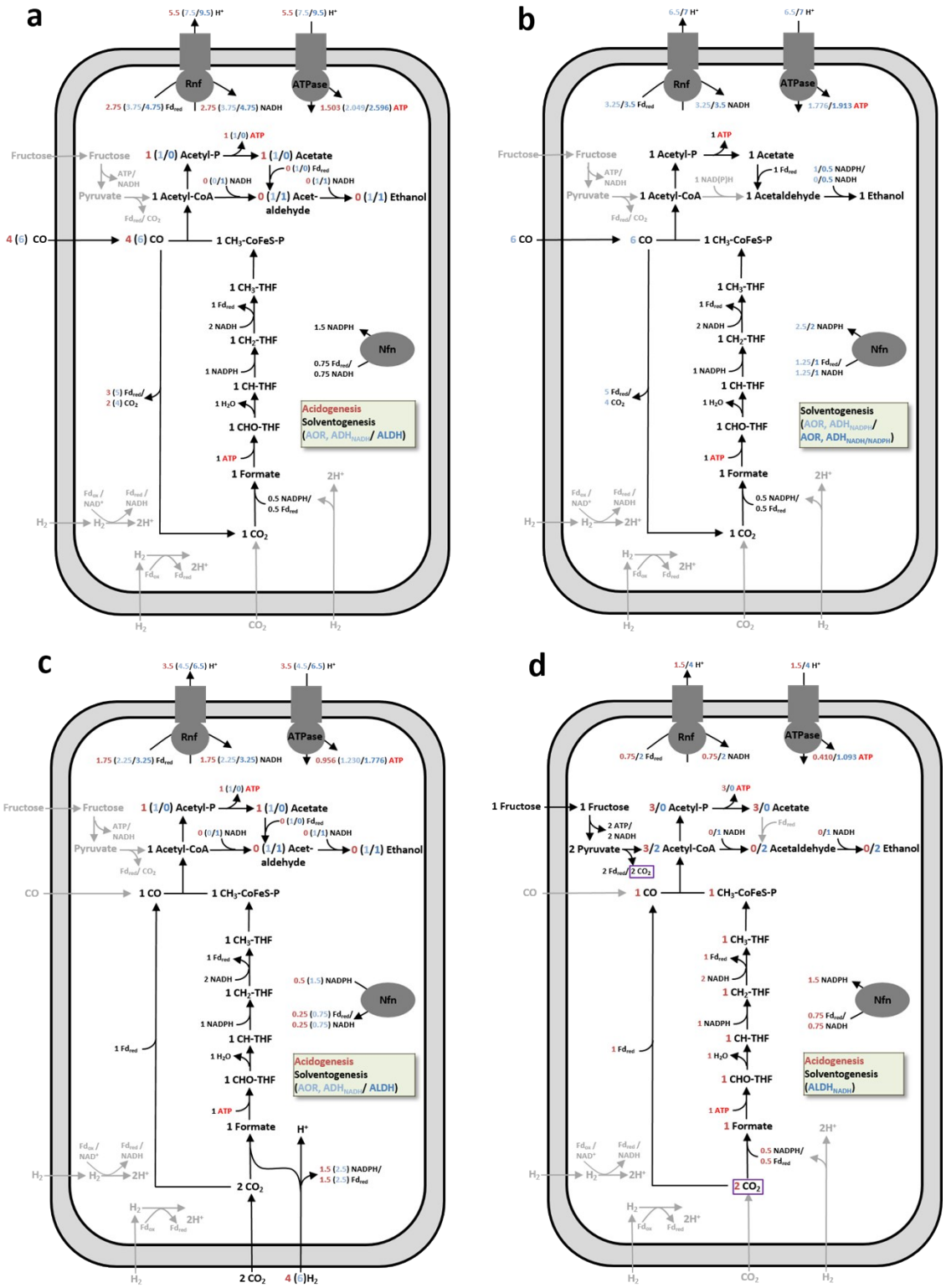

658 **Figure S2**

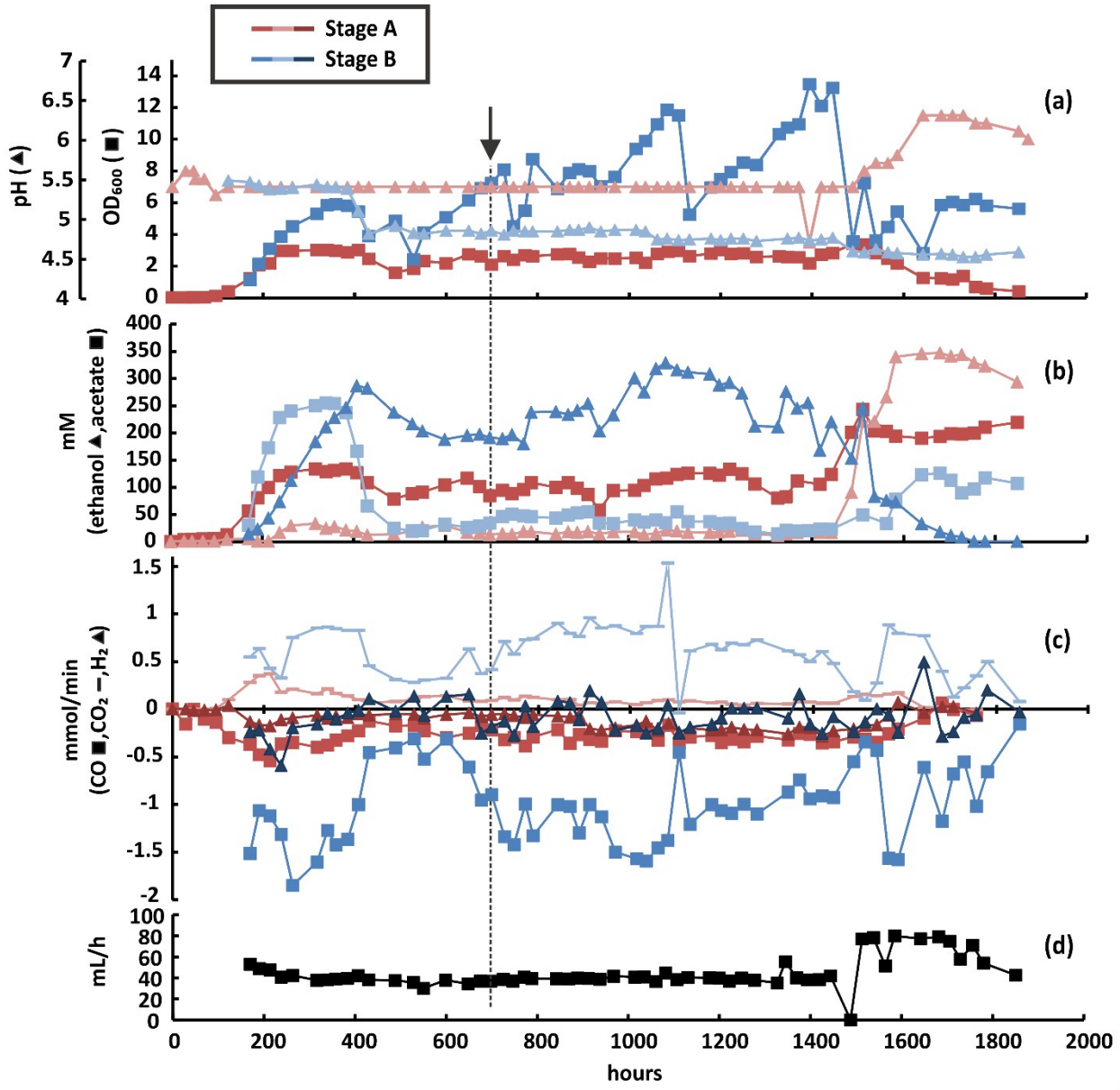

659

660

661 **Figure S3**

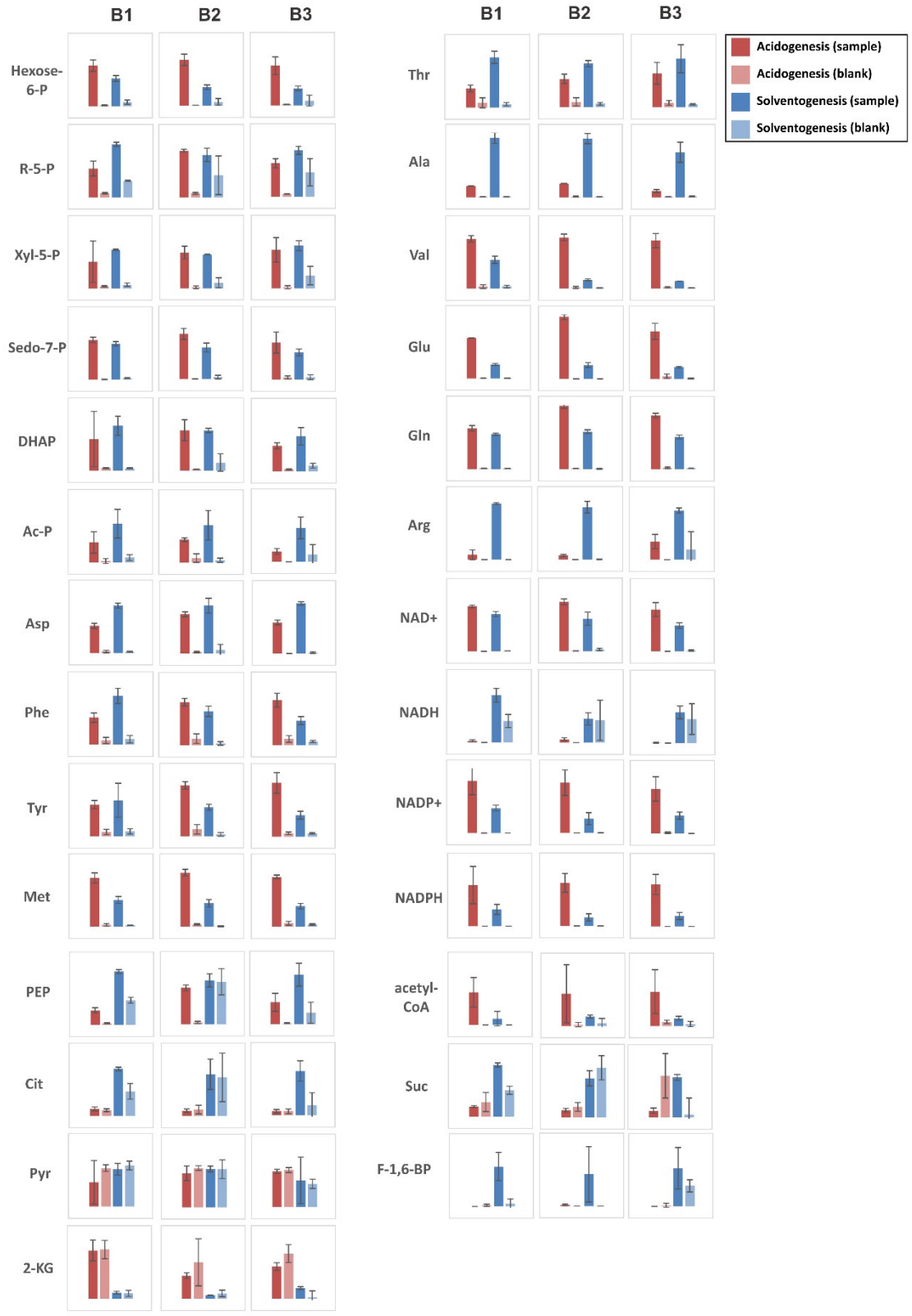

662

Supplemental Tables

Energy Source/ Fermentation product	AOR/ALDH	ADH specificity	NADPH produced at Nfn-complex	Stoichiometry at Rnf-complex (Fd_{red} -> NADH)	Net ATP gain/mol product	Net ATP gain/ mol substrate (CO, H_2 or fructose)	CO_2 produced/ mol product	CO_2 produced/ mol substrate
CO								
Acetate			1.5	2.75	1.503	0.376	2	0.5
Ethanol	ALDH	NADH	1.5	4.75	1.596	0.266	4	0.67
Ethanol	AOR	NADH	1.5	3.75	2.049	0.342	4	0.67
Ethanol	AOR	NADH/NADPH	2	3.5	1.913	0.319	4	0.67
Ethanol	AOR	NADPH	2.5	3.25	1.776	0.296	4	0.67
H_2/CO_2								
Acetate			-0.5*	1.75	0.956	0.239	-	-
Ethanol	ALDH	NADH	-1.5*	3.25	0.776	0.129	-	-
Ethanol	AOR	NADH	-1.5*	2.25	1.230	0.205	-	-
fructose								
Acetate			1.5	0.75	1.470	4.410	-	-
Ethanol	ALDH	NADH	1.5	2	1.547	3.093	0.67	2

Table S1. Stoichiometries of enzyme complexes, net ATP yields and CO_2 production from different energy sources considering different scenarios.

* NADPH is consumed; AOR, aldehyde:ferredoxin oxidoreductase route; ALDH, aldehyde dehydrogenase route

	At sampling time for			
	Proteomics		Metabolomics*	
	Stage A	Stage B	Stage A	Stage B
Concentrations				
Acetate (mM)	82.97	33.09	83.93 [8.22]	60.74 [9.17]
Ethanol (mM)	12.10	188.23	8.3 [0.95]	428.55 [12.19]
OD_{600}	2.12	7.25	1.77 [0.23]	21.18 [0.22]
Cell density (mgDW/L)	512.56	1754.50	429.07 [56.47]	5124.59 [53.05]
Acetate normalized (mM/OD_{600})	39.17	4.56	47.34 [1.61]	2.87 [0.46]
Ethanol normalized (mM/OD_{600})	5.71	25.96	4.68 [0.08]	20.24 [0.37]
Molar Ratio Ethanol:Acetate	0.15	5.69	0.099 [0.002]	7.15 [1.28]
Rates for system				
Flow rate (mL/h)	36.85	36.85	38.16 [2.24]	76.32 [4.48]
Dilution rate (1/h)	0.037	0.009	0.038 [0.002]	0.019 [0.001]
Acetate production/consumption rate				
Normalized to volume (mmol/h*L)	3.058	-0.688**	3.203 [0.502]	-0.512 [0.065]
Normalized to cell density (mmol/h*L*OD)	1.444	-0.095	1.806 [0.045]	-0.024 [0.003]
Ethanol production rate				
Normalized to volume (mmol/h*L)	0.446	0.322	0.317 [0.055]	1.963 [0.048]
Normalized to cell density (mmol/h*L*OD)	0.211	0.044	0.179 [0.007]	0.093 [0.003]

Table S2. Growth data summary at the time-points of sampling for proteome and metabolome analyses

*data for metabolomics reactor as average [SD] for three sampling time points within 24 h (*n=3*)

**negative values indicate net consumption

Table S3. Most abundant proteins in proteome analysis

Accession (CLJU_)	Annotation (revised, commented)	Function	µmol/mol	Fold-change (sol./acid.)
c39950	predicted NADPH-dependent butanol dehydrogenase	Energy	55477	-2.2
c39340	predicted rubrerythrin (reverse rubrerythrin; Hsp21)	Stress	47230	1.1
c33240	predicted cold shock protein CspA (ssDNA-/ssRNA-binding)	Stress; Regulation	45746	-1.2
c13850	pyridoxamine 5'-phosphate oxidase; flavin reductase (also: nicotinate phosphoribosyltransferase)	Vitamin; Cofactor	37721	1.7
c41790	predicted stage V sporulation protein G (DNA-binding protein)	Sporulation/ Germination; Regulation; Cell cycle; Stress	36704	1.6
c24260	putative cyclase (Kynurenine formamidase)	aa (aromatic)	27027	26.4
c37580	CO dehydrogenase/acetyl-CoA synthase, delta subunit	Energy (WLP)	24049	1.2
c37560	predicted methyltetrahydrofolate:corrinoid/iron-sulfur protein methyltransferase (AcsE)	Energy (WLP)	21989	-1.1
c37650	formate-tetrahydrofolate ligase	Energy (WLP)	21153	-1.4
c00680	predicted hydroxyacid dehydrogenase/reductase (2-hydroxy-3-oxopropionate reductase)	General metabolism	20664	-1.2
c37570	CO dehydrogenase/acetyl-CoA synthase gamma subunit	Energy (WLP)	16316	-1.2
c37620	methylenetetrahydrofolate reductase subunit (MetV)	Energy (WLP)	16278	-1.1
c04840	predicted cell wall binding protein	Cell envelope; Stress	15507	2.0
c20210	predicted tungsten-containing aldehyde ferredoxin oxidoreductase (AOR)	Energy	15419	-2.5
c20110	predicted tungsten-containing aldehyde ferredoxin oxidoreductase (AOR)	Energy	13639	-1.5
c39310	cysteine synthase	aa (sulfur)	12324	26.7
c37190	60 kDa chaperonin (GroEL)	Stress	10439	3.7
c37550	CO dehydrogenase/acetyl-CoA synthase complex beta subunit	Energy (WLP)	9047	-1.4
c18160	pyrimidine-nucleoside phosphorylase	DNA	7658	1.0
c06640	O-acetylhomoserine sulfhydrylase	aa (sulfur)	7657	37.6
c12780	acetate kinase	Energy	7399	-1.2
c32100	putative ABC-type metal ion transport system, periplasmic component	Transport	7348	13.9
c37670	carbon monoxide dehydrogenase	Energy (WLP)	7047	-1.1
c07040	NADP-specific electron-bifurcating [FeFe] hydrogenase subunit (HytB)	Energy (WLP)	6631	-1.8
c11380	predicted electron transport complex protein RnfG	Energy	6402	-1.2
c39580	pyridoxal biosynthesis protein PdxS	Vitamin	6369	3.5
c12120	NifU protein, N-terminal	Nitrogen	6357	2.6
c24190	NADPH-dependent glutamate synthase beta chain	Nitrogen; aa	5072	1.8
c37600	dihydrolipoamide dehydrogenase	General metabolism	4852	-1.2
c39150	glyceraldehyde-3-phosphate dehydrogenase	Central metabolism	4793	-1.2
c41130	50S ribosomal protein L7/L12	Translation	4580	-1.0
c22210	bifunctional AICARFT /IMPCHase (bifunctional enzymes catalyzing the last two steps in de novo purine biosynthesis)	DNA	4389	1.3
c00960	predicted aminotransferase (serine-pyruvate aminotransferase)	aa	4272	12.9
c20390	ketol-acid reductoisomerase (ilvC2)	aa	3950	-1.4
c13400	glyceraldehyde-3-phosphate dehydrogenase	Central metabolism	3911	-2.5
c11360	predicted electron transport complex protein RnfC	Energy	3731	-1.5
c07070	NADP-specific electron-bifurcating [FeFe] hydrogenase subunit (HytA)	Energy (WLP)	3602	-1.5
c18120	cytidine deaminase	DNA	3556	1.3
c02430	F1Fo ATPase, subunit beta	Energy	3327	1.2
c37520	conserved hypothetical protein (RNA-binding)	Unknown	3323	1.6
c09340	pyruvate:ferredoxin oxidoreductase	Central metabolism	3318	-1.2
c37640	formyltetrahydrofolate cyclohydrolase	Energy (WLP)	3204	-1.2
c07080	NADP-specific electron-bifurcating [FeFe] hydrogenase subunit (HytE2)	Energy (WLP)	3171	-1.1
c37310	conserved hypothetical protein (ferredoxin-like fold)	Unknown	3153	-1.6
c41060	elongation factor Tu	Translation	3151	-1.0
c25040	putative molybdenum cofactor sulfurase related protein	Cofactor/ Nitrogen	3131	-1.5
c05110	predicted cell wall binding protein	Cell envelope; Stress	3129	-1.3
c40920	50S ribosomal protein L5	Translation	2927	1.0
c00670	hydroxyacid dehydrogenase/reductase related protein (2-hydroxy-3-oxopropionate reductase- related)	General Metabolism	2897	-1.8
c41080	30S ribosomal protein S7	Translation	2848	1.1
c23480	S-Ribosylhomocysteinase (LuxS; AI-2 biosynthesis; SAM metabolism; methionine metabolism)	Signaling (cell-cell); general metabolism; aa (sulfur)	2796	6.6
c12110	homocysteine desulfhydrase (cysteine desulfurase NifS)	Nitrogen	2778	3.1
c18130	deoxyribose-phosphate aldolase	DNA	2691	-1.2
c41490	predicted transcription elongation factor	Transcription	2663	1.3

Accession (CLJU_)	Annotation (revised, commented)	Function	µmol/mol	Fold-change (sol./acid.)
c34560	dihydrodipicolinate synthase (lysine biosynthesis)	aa	2650	1.3
c11220	spo0A-like protein	Sporulation/ Germination; Stress	2575	-1.5
c35240	putative nitroreductase	Energy/ Cofactor	2556	1.1
c37630	bifunctional protein: methylenetetrahydrofolate dehydrogenase /methenyltetrahydrofolate cyclohydrolase	Energy (WLP)	2546	-1.2
c24130	predicted aldehyde oxidoreductase (aerobic-type CODH)	Energy	2542	1.4
c12100	putative transcriptional regulator (Rrf2 familiy)	Regulation	2516	2.7
c21680	conserved hypothetical protein (inosine-5'-monophosphate dehydrogenase)	DNA	2514	1.3

Table S4. Up-regulated proteins in solventogenesis (sol.) *vs.* acidogenesis (acid.)

Accession (CLJU_)	Annotation (revised)	Function	µmol/mol	Fold-change (sol./acid.)
c06640	O-acetylhomoserine sulfhydrylase	aa (sulfur)	7657	37.6
c18340	conserved hypothetical protein (thioredoxin or arylsulfotransferase)	Signaling (redox, cell-cell)	1063	31.2
c21200	predicted aluminum resistance protein (cystathionine beta-lyase)	aa (sulfur); Nitrogen	13	29.5
c39310	cysteine synthase	aa (sulfur)	12324	26.7
c24380	cystathione gamma-synthase (cystathionine beta-lyase)	aa (sulfur); Nitrogen	1042	26.4
c24260	putative cyclase (Kynurenine formamidase)	aa (aromatic)	27027	26.4
c18330	ABC-type nitrate/sulfonate/bicarbonate transport systems periplasmic components-like protein (aliphatic sulfonate transporter)	Transport (sulfur)	841	22.1
c24370	cysteine synthase	aa (sulfur)	2031	21.8
c23500	hypothetical protein	unknown	241	21.3
c23520	nitrogenase molybdenum-iron protein, alpha chain	Nitrogen	423	19.5
c23510	nitrogenase molybdenum-iron protein, beta chain	Nitrogen	495	14.8
c24250	predicted aminoacid permease	Transport	71	14.7
c32100	putative ABC-type metal ion transport system, periplasmic component	Transport	7348	13.9
c00960	predicted aminotransferase (serine-pyruvate aminotransferase)	aa	4272	12.9
c17080	conserved hypothetical protein (peptidase)	Protein digestion	42	11.9
c00980	uncharacterized conserved protein	unknown	648	11.8
c25140	conserved hypothetical protein (metallo beta lactamase superfamily)	Antibiotic resistance	17	9.5
c18320	predicted ABC nitrate/sulfonate/bicarbonate family transporter, ATPase component	Transport (sulfur)	434	9.3
c23530	nitrogenase iron protein (NifH)	Nitrogen	884	8.8
c15890	hypothetical protein	unknown	40	7.5
c24330	homoserine O-succinyltransferase (*metA*)	aa (sulfur)	1238	7.1
c23480	S-Ribosylhomocysteinase (LuxS; AI-2 biosynthesis; SAM metabolism; methionine metabolism)	Signaling (cell-cell); general metabolism; aa (sulfur)	2796	6.6
c26570	glycerol dehydrogenase	Central metabolism	1513	6.0
c04600	predicted ABC transporter, ATPase component (D-methionine transporter)	Transport (sulfur)	880	5.9
c18310	predicted ABC nitrate/sulfonate/bicarbonate family transporter, permease component	Transport (sulfur)	161	5.7
c42690	18 kDa heat shock protein (Hsp18a)	Stress	164	5.1
c42700	18 kDa heat shock protein (Hsp18b)	Stress	126	5.1
c18470	predicted iron-containing alcohol dehydrogenase (NADPH-dependent BDH)	Energy	829	4.9
c00970	D-3-phosphoglycerate dehydrogenase (first step in serine biosynthesis)	aa (sulfur related)	372	4.8
c01550	hypothetical protein	unknown	36	4.7
c39300	serine acetyltransferase	aa (sulfur related)	120	4.7
c29110	shikimate kinase	aa (aromatic)	218	4.4
c05030	putative membrane protein (ABC-2 type transport system permease protein)	Transport	11	4.3
c08430	predicted serine protease (participates in heat-shock response)	Stress	231	4.3
c33060	thiamine-phosphate pyrophosphorylase	Vitamin	496	4.0
c11200	predicted DNA repair protein RecN (ATPase involved in DNA repair)	DNA	29	3.8
c37200	10 kDa chaperonin (Cpn10 or GroES)	Stress	1882	3.8
c24780	predicted flavodoxin (multimeric flavodoxin WrbA; NAD(P)H-dependent FMN-reductase)	Stress	267	3.7
c38220	conserved hypothetical protein	unknown	70	3.7
c37190	60 kDa chaperonin (GroEL)	Stress	10439	3.7
c33260	L-serine dehydratase, beta chain SdhB	aa (sulfur related)	12	3.7
c04610	predicted ABC-type metal ion transport system, permease component (methionine transporter)	Transport (sulfur)	112	3.6
c39580	pyridoxal biosynthesis protein PdxS	Vitamin	6369	3.5
c21730	ABC transporter, periplasmic component (spermidine/putrescine; thiamine)	Stress; Vitamin	51	3.5
c33050	hydroxyethylthiazole kinase (4-methyl-5-beta-hydroxyethylthiazole (Thz) kinase, thiamine metabolism)	Vitamin	298	3.3
c22100	predicted methyl-accepting chemotaxis transducer protein	Chemotaxis	16	3.3
c04990	putative surface-layer protein (putative cell wall-binding protein)	Stress	262	3.3
c01640	radical SAM domain protein	Energy; Cofactor	100	3.1
c12110	homocysteine desulfhydrase (cysteine desulfurase NifS)	Nitrogen	2778	3.1
c04310	predicted Na+/H+-dicarboxylate symporter	Transport/ Energy	7	3.1
c32210	hypothetical protein (peptidase)	Protein digestion	22	3.0
c19590	predicted transcriptional regulator (aminotransferase)	aa	680	3.0
c06650	methionine synthase	aa (sulfur)	264	3.0
c05070	conserved hypothetical protein (“outer membrane” protein TolC)	Stress	114	3.0
c21880	putative aminopeptidase 1	Protein digestion	463	2.9

Accession (CLJU_)	Annotation (revised)	Function	µmol/mol	Fold-change (sol./acid.)
c05940	putative polyprotein (Macro domain, Af1521- and BAL-like family)	DNA; Regulation	31	2.9
c21080	predicted cobalamin B12-binding protein (methyltransferase; methionine synthase domain)	Cofactor; aa (sulfur)	78	2.8
c36060	hypothetical protein	Unknown	160	2.8
c04620	conserved hypothetical protein	Unknown	112	2.8
c19320	predicted amino acid permease	Transport	17	2.8
c04080	putative membrane protein (RND family efflux transporter)	Transport	36	2.8
c21210	predicted RNA-binding protein Hfq	Regulation	902	2.7
c34270	hypothetical protein	unknown	65	2.7
c21720	predicted aminohydrolase (glutamate deacylase)	aa	41	2.7
c17750	putative membrane protein	unknown	42	2.7
c12100	putative transcriptional regulator	Regulation	2516	2.7
c06300	putative ABC-type transporter, periplasmic component	Transport	56	2.7
c33870	conserved hypothetical protein	unknown	133	2.7
c12120	NifU protein, N-terminal	Nitrogen	6357	2.6
c08840	predicted Beta-lactamase:Copper amine oxidase-like protein (peptidoglycan-binding protein)	Antibiotic resistance; cell envelope	101	2.6
c23270	putative secretion protein	Transport	214	2.6
c01630	B3/4 domain protein	Regulation	217	2.6
c11860	predicted two-component sensor kinase	Regulation	13	2.6
c39540	potassium-transporting ATPase, c-chain	Transport	45	2.5
c07150	homoserine dehydrogenase (Hom1)	aa (sulfur related)	423	2.5
c21060	predicted methyltransferase MtaA/CmuA family	Cofactor	8	2.5
c05980	signal peptidase	Regulation; Transport	270	2.5
c09460	chemotaxis protein	Chemotaxis	1322	2.5

Table S5. Down-regulated proteins in solventogenesis (sol.) *vs.* acidogenesis (acid.)

Accession (CLJU_)	Annotation (revised, commented)	Function	µmol/mol	Fold-change (sol./acid.)
c21580	predicted electron transfer flavoprotein alpha subunit (EtfA)	Energy	29	-21.5
c24240	predicted NADH oxidase , Old yellow enzyme (OYE) -like FMN-binding domain	Energy	27	-16.4
c10550	conserved hypothetical protein	Unknown	16	-16.0
c21430	predicted methyl-accepting chemotaxis protein	Chemotaxis	4	-10.6
c40060	predicted ABC transporter, ATPase component	Transport	5	-9.8
c33820	Holliday junction DNA helicase	DNA	16	-9.4
c03780	putative patatin-like phospholipase	Energy storage; cell envelope	26	-9.1
c16520	bifunctional aldehyde/alcohol dehydrogenase (AdhE1)	Energy	6	-8.1
c15770	predicted transcriptional regulator, DeoR family	Regulation	22	-7.7
c23180	predicted symporter (Na^+/glucose)	Transport	26	-6.0
c17220	predicted ABC transporter, ATPase component	Transport	8	-6.0
c01990	predicted glycosyltransferase	Cell envelope	7	-5.9
c35180	predicted two-component sensor histidine kinase	Regulation	17	-5.8
c42380	Small GTP-binding protein domain protein (ribosome-associated)	Translation	124	-5.1
c20130	sigma-54- interacting transcription regulator	Regulation	44	-5.0
c19870	putative membrane protein (L-cysteine desulfidase CdsB)	aa (sulfur)	193	-4.7
c27710	L-seryl-tRNA(Sec) selenium transferase (selenocystein synthase)	aa	6	-4.5
c12010	alanine racemase	aa	22	-4.5
c15710	conserved hypothetical protein	Unknown	8	-4.4
c40080	hypothetical protein	Unknown	14	-4.3
c15450	MarR family transcriptional regulator	Regulation	17	-4.1
c14470	hypothetical protein (DnaJ/Hsp40 domain)	Translation	18	-4.1
c00880	conserved hypothetical protein	Unknown	25	-4.1
c16200	conserved hypothetical protein (ecf-type sigma 70 factor negative-effector)	Stress	28	-4.1
c08850	predicted transcriptional regulator with a HTH and aminotransferase domain	Regulation	6	-4.0
c37960	conserved hypothetical protein	Unknown	105	-4.0
c39650	putative membrane protein	Unknown	177	-4.0
c27590	hypothetical protein	Unknown	11	-3.7
c01410	DNA polymerase related protein (DNA polymerase subunit delta)	DNA	59	-3.7
c36580	hypothetical protein (DNA ligase-like)	DNA	22	-3.5
c26470	predicted anion permease	Transport	7	-3.5
c21810	predicted amino acid permease	Transport	41	-3.4
c29470	conserved hypothetical protein	Unknown	19	-3.4
c42490	agmatine deiminase	aa	119	-3.3
c08500	predicted spore germination protein	Sporulation/ Germination	7	-3.3
c30810	non-heme chloroperoxidase (hydrolase of unknown function)	Unknown	10	-3.3
c32090	predicted phosphatase (protein tyrosine phosphatase)	Regulation	7	-3.2
c42560	ornithine carbamoyltransferase	aa	148	-3.1
c18060	predicted transcriptional regulator	Regulation	12	-3.1
c30710	hypothetical protein	Unknown	111	-3.1
c07510	putative cobalamin B12-binding methyltransferase	Cofactor; aa (sulfur)	177	-3.0
c07530	putative metal binding protein	Cofactor	9	-2.9
c08520	putative hydrolase	Unknown	758	-2.8
c33380	predicted molybdenum cofactor biosynthesis protein A	Cofactor	394	-2.8
c06610	(Re)-citrate-synthase	Central metabolism	240	-2.8
c14370	sensor protein VanS	Regulation	14	-2.7
c18520	putative recombinase	DNA	5	-2.7
c12710	conserved hypothetical protein (DNA methylation or Methyl transfer for pantothenate synthesis)	Vitamin; Regulation	93	-2.7
c03800	hypothetical protein	Unknown	17	-2.7
c20020	conserved hypothetical protein	Unknown	164	-2.6
c12330	predicted RNA polymerase sigma-G factor	Sporulation/ Germination	35	-2.6
c18350	predicted ABC transporter, ATP-binding component	Transport	28	-2.6
c12910	predicted 16S rRNA processing protein RimM	Translation	56	-2.6
c16610	putative DNA-binding protein	Regulation	23	-2.5
c20210	predicted tungsten-containing aldehyde ferredoxin oxidoreductase	Energy	15419	-2.5
c35270	putative transporter protein	Transport	43	-2.5
c13400	glyceraldehyde-3-phosphate dehydrogenase	Central Metabolism	3911	-2.5

Table S6. List of enzymes in central anabolism depicted in Figure 2.

Accession (CLJU_)	µmol/mol	Fold-change (sol./acid.)
Pyruvate metabolism		
#1: Pyruvate:ferredoxin oxidoreductase		
c09340	3318	-1.2
c29340	ND*	ND
#2: Pyruvate-formate lyase		
c11830	6	-1.6
c11840	18	-1.6
c25970	ND	ND
c25980	ND	ND
c39820	ND	ND
c39830	ND	ND
#3: Pyruvate kinase		
c03260	519	1.0
#4(1): Pyruvate-phosphate dikinase		
c08140	963	-1.3
#4(2): Posphoenolpyruvate synthase (Pyruvate,water dikinase)		
c14340	9	-1.6
c38600	6	-1.3
#5: Pyruvate carboxylase		
c37390	1023	-1.2
#6: Phosphoenolpyruvate carboxykinase		
c06210	280	-1.3
#7: Malic enzyme		
c04160	145	-1.2
c25360	ND	ND
c30500	ND	ND
c38460	6	NQ**
Branched TCA cycle		
#8: Malate dehydrogenase		
c05920	152	-1.0
#9: Fumarase		
c40590	123	1.0
c40600	173	1.0
#10: Fumarate reductase/ succinate dehydrogenase		
c08670	ND	ND
c22800	ND	ND
c22820	ND	ND
c30250	15	-1.0
#11: Citrate lyase		
c40560	110	-1.3
c40570	105	-1.1
c40580	30	-1.4
c25320	5	-1.1
c25330	ND	ND
c25340	ND	ND
c30470	ND	ND
c30480	ND	ND

Accession (CLJU_)	µmol/mol	Fold-change (sol./acid.)
c30490	ND	ND
#12: Citrate synthase		
c06610	240	-2.8
#13: Aconitase		
c06620	198	1.3
c24200	11	1.6
c30460	ND	ND
#14: Isocitrate dehydrogenase		
c06630	368	1.0
Gluconeogenesis/ Glycolysis		
#15: Enolase		
c39110	1543	-1.0
#16: Phosphoglyceromutase		
c26320	69	-1.2
c39120	163	-1.2
#17: Phosphoglycerate kinase		
c39140	697	1.2
#18: Glyceraldehyde 3-phosphate dehydrogenase		
c13400	3910	-2.5
c39150	4793	-1.2
#19: Triosephosphate isomerase		
c39130	833	-1.2
#20: Fructose 1,6-bisphosphate aldolase		
c00660	1462	-1.7
c02810	1526	1.1
#21: Fructose 1,6-bisphosphatase		
c29050	208	-1.6
#22: phosphofructokinase		
c03250 (6-P-fructose)	372	-1.1
c25790 (6-P-fructose)	ND	ND
c20600 (1-P-fructose)	9	NQ
#23: Phosphoglucose isomerase		
c37130	111	-1.3
Pentose phosphate pathway		
#24: Transaldolase		
c39640	1814	-1.1
#25: Transketolase		
c03050	498	1.4
c03060	328	-1.2
c25820	18	-1.1
c25830	19	NQ
#26: Ribulose 5-phosphate isomerase		
c02310	537	-1.5
#27: Ribulose 5-phosphate 3-epimerase		
c12640	130	1.7
#28: 6-phosphogluconate dehydrogenase		
c11590	42	2.1

*ND, not detected; **NQ, not quantified

Table S7. List of metabolites in central anabolism, depicted in Figures 2 and 3.

Compound name (abbreviation)	Sample Acidogenesis (mean [SD]*)	Blank Acidogenesis (mean [SD]*)	Sample/Blank Acidogenesis	Sample Solventogenesis (mean [SD]*)	Blank Solventogenesis (mean [SD]*)	Sample/Blank Solventogenesis	p-value**
Hexose-6-phosphate (Hexose-6-P)	5483465 [1581295]	83595 [34221]	66	2646538 [452707]	526173 [466030]	5	
Ribose-5-phosphate (R-5-P)	899753 [196074]	91115 [26898]	10	1191159 [233261]	520119 [285522]	2	
Xylulose-5-phosphate (Xyl-5-P)	210248 [112858]	9594 [10067]	22	249523 [90919]	40026 [26357]	6	
Sedoheptulose-7-phosphate (Sedo-7-P)	691327 [160679]	14560 [20732]	47	533562 [93168]	34864 [26728]	15	0.2054
Dihydroxyacetone-phosphate (DHAP)	92824 [47863]	6023 [2354]	15	114902 [25276]	15620 [14252]	7	
Acetyl-phosphate (Ac-P)	43355 [23609]	5640 [9900]	8	89291 [40456]	11920 [15514]	7	
Asp	4815309 [1102258]	162891 [166317]	30	7148219 [879715]	284003 [488452]	25	0.0640
Phe	1822326 [460056]	270115 [165946]	7	1700376 [560683]	174836 [126164]	10	
Tyr	2156764 [560680]	231752 [151864]	9	1369142 [515844]	160877 [99129]	9	
Met	322389 [25324]	16681 [9346]	19	150017 [24953]	9404 [5864]	16	0.0004
Thr	1497767 [498719]	267559 [191201]	6	2627760 [462235]	175652 [62506]	15	
Ala	4164564 [1341519]	266735 [139756]	16	21554824 [3724703]	296500 [118976]	73	0.0034
Val	8640255 [3638043]	240675 [158438]	36	1975178 [318738]	152821 [62706]	13	0.1060
Glu	63421870 [13132355]	1425289 [2075722]	44	16840884 [2077507]	293811 [441055]	57	0.0285
Gln	12484230 [2397661]	239268 [155096]	52	8278199 [620767]	167908 [104399]	49	0.1192
Pro	1227535 [215288]	369574 [146087]	3	7857639 [841069]	5658103 [4406756]	1	
Arg	6653 [3964]	0 [0]	6653	53550 [23031]	1705 [4848]	31	0.0907
NAD+	14381725 [1576069]	52805 [26861]	272	10099581 [1986945]	332592 [267277]	30	0.0430
NADH	18318 [17020]	0 [0]	18318	348870 [122083]	232070 [135040]	2	
NADP+	2133666 [511768]	11781 [21444]	181	830561 [263843]	3296 [9887]	252	0.0015
NADPH	132882 [36883]	0 [0]	132882	37498 [16688]	0 [0]	37498	0.0076
Phophoenolpyruvate (PEP)	655140 [291484]	39702 [22648]	17	1315420 [210310]	868894 [314752]	1.51	
Pyruvate (Pyr)	347547 [140386]	424067 [28287]	0.82	378191 [146965]	427739 [66394]	0.88	
Citrate (Cit)	439868 [143676]	445457 [263248]	0.99	3604702 [967576]	2566732 [1591589]	1.40	
2-Ketoglutarate (2-KG)	12025742 [6080338]	15063410 [7753348]	0.80	2028166 [425387]	2113003 [1206493]	0.96	
Succinate (Suc)	47506494 [12197322]	136088923 [123422008]	0.35	257389922 [34683491]	217071293 [90987514]	1.19	
Acetyl-CoA	43878 [27260]	2680 [3511]	16	10313 [5191]	1875 [3787]	5.50	
Fructose-1,6-bisphosphate (F-1,6-BP)	2404 [4805]	4075 [6133]	0.59	196349 [117095]	10028 [20362]	20	

* values depicted in this table show sample and blank values separately, averages for 3 biological replicates with 3 technical replicates each (*n = 9*) ; peak area top values, no absolute quantification; compare only acidogenesis and solventogenesis for each compound and not compounds with each other.

** t-test performed on values with a “sample to blank” ratio of ≥ 10 for both acidogenesis and solventogenesis; the averages of the three technical replicates for each biological replicate were used for the statistical test (*n=3*).

666

667 **Table S8. List of metabolites in central anabolism. This table gives values for sample and blank for all three biological replicates (B1-B3) separately (with**
668 **three technical replicates each).**

Compound name (abbreviation)	Sample Acidogenesis (mean [SD]*)	Blank Acidogenesis (mean [SD]*)	Sample Solventogenesis (mean [SD]*)	Blank Solventogenesis (mean [SD]*)
B1				
Hexose-6-phosphate (Hexose-6-P)	4161669 [587326]	79597 [30584]	2851503 [296448]	403825 [220384]
Ribose-5-phosphate (R-5-P)	797708 [203567]	113867 [19302]	1469267 [59472]	456272 [14332]
Xylulose-5-phosphate (Xyl-5-P)	253515 [196684]	20171 [5986]	367080 [5752]	35437 [16520]
Sedoheptulose-7-phosphate (Sedo-7-P)	629678 [42522]	4542 [4123]	568811 [32432]	24294 [7706]
Dihydroxyacetone-phosphate (DHAP)	95415 [83032]	8692 [1333]	135401 [28578]	7832 [1112]
Acetyl-phosphate (Ac-P)	28361 [15238]	2052 [3554]	55084 [20485]	6904 [4156]
Asp	4322201 [391501]	250488 [195896]	7522944 [403187]	184832 [97517]
Phe	1285485 [229098]	202373 [150423]	2321619 [363513]	266830 [174908]
Tyr	1512439 [192761]	209620 [124112]	1711884 [806662]	237221 [121433]
Met	308568 [32477]	11725 [8619]	170233 [21817]	9685 [513]
Thr	1054801 [186140]	265736 [271333]	2782798 [337742]	181799 [93267]
Ala	4498747 [128151]	207866 [111230]	23532137 [2200972]	251949 [95878]
Val	3946512 [254042]	176398 [145980]	2292752 [286116]	169980 [103281]
Glu	51307727 [305515]	449913 [187650]	17727742 [1293006]	145729 [175651]
Gln	9641052 [652540]	164520 [39241]	8251679 [271105]	116795 [23589]
Pro	1126924 [129773]	412947 [130238]	7563368 [442949]	2328257 [499652]
Arg	6140 [6269]	0 [0]	70935 [1230]	0 [0]
NAD+	14287574 [439527]	67817 [12006]	11872011 [774165]	166320 [36893]
NADH	17088 [10943]	0 [0]	486628 [70422]	219883 [66732]
NADP+	2272587 [605059]	4474 [7749]	1090209 [126847]	0 [0]
NADPH	130077 [59171]	0 [0]	53427 [16234]	0 [0]
Phophoenolpyruvate (PEP)	392509 [70935]	42943 [15949]	1435552 [54665]	664113 [78785]
Pyruvate (Pyr)	269332 [240037]	426529 [36677]	413537 [64450]	455760 [48549]
Citrate (Cit)	439336 [121188]	357618 [95164]	2978985 [106666]	1558150 [496683]
2-Ketoglutarate (2-KG)	19049688 [4091475]	19419165 [3637491]	2391277 [518490]	2128499 [1190267]
Succinate (Suc)	56561245 [5683341]	81532405 [52170444]	286502193 [11442082]	146550060 [22126111]
Acetyl-CoA	38941 [17739]	0 [0]	7508 [8707]	0 [0]
Fructose-1,6-bisphosphate (F-1,6-BP)	0 [0]	8056 [7047]	253777 [89834]	17921 [31040]

Compound name (abbreviation)	Sample Acidogenesis (mean [SD]*)	Blank Acidogenesis (mean [SD]*)	Sample Solventogenesis (mean [SD]*)	Blank Solventogenesis (mean [SD]*)
B2				
Hexose-6-phosphate (Hexose-6-P)	7249538 [896339]	54574 [10968]	2918443 [366025]	595666 [522567]
Ribose-5-phosphate (R-5-P)	1110005 [33348]	94439 [24912]	1005939 [156451]	524084 [457323]
Xylulose-5-phosphate (Xyl-5-P)	225577 [39734]	5161 [8939]	213420 [1605]	34844 [31084]
Sedoheptulose-7-phosphate (Sedo-7-P)	856558 [103153]	3455 [3042]	599008 [86106]	38073 [33686]
Dihydroxyacetone-phosphate (DHAP)	112683 [29045]	4086 [504]	112206 [5966]	23384 [24145]
Acetyl-phosphate (Ac-P)	72356 [6188]	14868 [13587]	118419 [46435]	7808 [6790]
Asp	6202466 [397136]	238185 [111609]	7586177 [1180761]	562992 [869363]
Phe	2048982 [178952]	318604 [229026]	1620430 [245721]	91101 [85857]
Tyr	2409430 [178530]	330730 [222451]	1376798 [140492]	89856 [84535]
Met	342352 [21077]	15366 [4078]	148766 [23413]	3435 [2988]
Thr	1555642 [263418]	290678 [229346]	2406518 [174903]	180664 [71937]
Ala	5476966 [70167]	299596 [216602]	23268125 [2000328]	238168 [77766]
Val	11335445 [734920]	246029 [198634]	1943468 [219284]	132549 [48158]
Glu	78519950 [3450683]	283731 [235767]	17596260 [2952759]	107638 [95091]
Gln	15023841 [588097]	169284 [34231]	8886949 [456665]	94751 [83989]
Pro	1412904 [92579]	489154 [60913]	7768947 [1199369]	9654486 [5463347]
Arg	5138 [1419]	0 [0]	66332 [7427]	243 [420]
NAD+	15605089 [915471]	61059 [37866]	10241050 [2056996]	524287 [390460]
NADH	34800 [15877]	0 [0]	244751 [63004]	229372 [206944]
NADP+	2188981 [555092]	0 [0]	625140 [263488]	9887 [17125]
NADPH	136312 [29586]	0 [0]	26424 [11581]	0 [0]
Phophoenolpyruvate (PEP)	982828 [75464]	51284 [32277]	1182051 [178923]	1145491 [352223]
Pyruvate (Pyr)	377877 [81426]	435239 [24990]	425274 [31299]	421958 [103452]
Citrate (Cit)	515636 [165338]	615196 [404696]	3966520 [1440798]	3665756 [2306050]
2-Ketoglutarate (2-KG)	10945340 [1355542]	17209033 [11206293]	1673334 [69330]	2489669 [1547732]
Succinate (Suc)	42627355 [10821460]	61840209 [25925075]	231285838 [45101686]	294565574 [71722132]
Acetyl-CoA	38306 [34602]	1576 [2729]	11165 [1888]	3283 [5686]
Fructose-1,6-bisphosphate (F-1,6-BP)	7212 [6351]	0 [0]	201592 [175210]	0 [0]
B3				
Hexose-6-phosphate (Hexose-6-P)	791547 [108335]	65040 [9374]	1098271 [95977]	580002 [324382]
Ribose-5-phosphate (R-5-P)	151651 [48713]	3451 [5978]	168069 [19820]	49796 [36395]
Xylulose-5-phosphate (Xyl-5-P)	587745 [167556]	35684 [26233]	432866 [52506]	42226 [37406]
Sedoheptulose-7-phosphate (Sedo-7-P)	70374 [8238]	5290 [1735]	97099 [24218]	15645 [6847]

Compound name (abbreviation)	Sample Acidogenesis (mean [SD]*)	Blank Acidogenesis (mean [SD]*)	Sample Solventogenesis (mean [SD]*)	Blank Solventogenesis (mean [SD]*)
Dihydroxyacetone-phosphate (DHAP)	29346 [8121]	0 [0]	94371 [30075]	21046 [26672]
Acetyl-phosphate (Ac-P)	3921260 [314452]	0 [0]	6335535 [223183]	104185 [95044]
Asp	2132511 [329269]	289367 [155261]	1159079 [192185]	166576 [48900]
Phe	2548424 [489722]	154905 [55447]	1018743 [182953]	155552 [32606]
Tyr	316246 [11195]	22951 [12651]	131053 [17655]	15091 [5126]
Met	1882857 [607495]	246264 [136097]	2693964 [770670]	164492 [38383]
Thr	2517978 [599467]	292742 [104908]	17864209 [3993665]	399383 [131993]
Ala	10638807 [1550019]	299597 [167919]	1689315 [32617]	155933 [40859]
Val	60437932 [10120370]	3542223 [2653262]	15198651 [890192]	628066 [696958]
Glu	12787799 [534117]	383999 [215313]	7695968 [440403]	292176 [29585]
Gln	1142778 [287197]	206620 [24317]	8240602 [912807]	4991567 [2515026]
Pro	8680 [3396]	0 [0]	23382 [1236]	4873 [8440]
Arg	13252511 [2175728]	29539 [7468]	8185682 [851141]	307168 [185387]
NAD+	3067 [5312]	0 [0]	315230 [65296]	246953 [158425]
NADH	1939429 [532232]	30870 [30732]	776333 [155253]	0 [0]
NADP+	132258 [32170]	0 [0]	32645 [10787]	0 [0]
NADPH	0 [0]	0 [0]	0 [0]	0 [0]
Phophoenolpyruvate (PEP)	590082 [241341]	24877 [14457]	1328659 [305496]	797077 [283916]
Pyruvate (Pyr)	395432 [24280]	410434 [27489]	295763 [256653]	405498 [51021]
Citrate (Cit)	364632 [153121]	363559 [198775]	3868600 [877166]	2476290 [1103702]
2-Ketoglutarate (2-KG)	6082198 [749116]	8562031 [1696747]	2019887 [251878]	1720843 [1251569]
Succinate (Suc)	43330882 [16150819]	264894155 [141131124]	254381736 [18430945]	210098245 [104596532]
Acetyl-CoA	54387 [34809]	6463 [2790]	12268 [3126]	2343 [4058]
Fructose-1,6-bisphosphate (F-1,6-BP)	0 [0]	4168 [7219]	133678 [72088]	12164 [21069]

669 * values depicted in this table show sample and blank values separately combining all three technical replicates (*n = 3*); peak area top values, no absolute
670 quantification; compare only acidogenesis and solventogenesis for each compound and not compounds with each other.

671 # Supplemental References

672 1. H. Richter, M. Martin and L. Angenent, *Energies*, 2013, **6**, 3987-4000.

673 2. M. E. Martin, H. Richter, S. Saha and L. T. Angenent, *Biotechnol. Bioeng.*, 2015, **113**, 531-539.

674 3. J. M. Perez, H. Richter, S. E. Loftus and L. T. Angenent, *Biotechnol. Bioeng.*, 2013, **110**, 1066-
675 1077.

676 4. M. M. Bradford, *Anal. Biochem.*, 1976, **72**, 248-254.

677 5. Q.-S. Yang, J.-H. Wu, C.-Y. Li, Y.-R. Wei, O. Sheng, C.-H. Hu, R.-B. Kuang, Y.-H. Huang, X.-X. Peng
678 and J. A. McCardle, *Mol. Cell. Proteomics*, 2012, **11**, 1853-1869.

679 6. Y. Wang, F. Yang, M. A. Gritsenko, Y. Wang, T. Clauss, T. Liu, Y. Shen, M. E. Monroe, D.
680 Lopez-Ferrer and T. Reno, *Proteomics*, 2011, **11**, 2019-2026.

681 7. S. Götz, J. M. García-Gómez, J. Terol, T. D. Williams, S. H. Nagaraj, M. J. Nueda, M. Robles, M.
682 Talón, J. Dopazo and A. Conesa, *Nucleic Acids Res.*, 2008, **36**, 3420-3435.

683 8. Y. Ishihama, Y. Oda, T. Tabata, T. Sato, T. Nagasu, J. Rappsilber and M. Mann, *Mol. Cell.*
684 *Proteomics*, 2005, **4**, 1265-1272.

685 9. L. Aristilde, I. A. Lewis, J. O. Park and J. D. Rabinowitz, *Appl. Environ. Microbiol.*, 2015, **81**, 1452-
686 1462.

687 10. S. S. Sasnow, H. Wei and L. Aristilde, *Microbiology Open*, 2016, **5**, 3-20.

688 11. W. Lu, M. F. Clasquin, E. Melamud, D. Amador-Noguez, A. A. Caudy and J. D. Rabinowitz,
689 *Analytical Chemistry*, 2010, **82**, 3212-3221.

690 12. M. F. Clasquin, E. Melamud and J. D. Rabinowitz, *Curr. Protoc. Bioinformatics.*, 2012, **Chapter 14**,
691 14.11. 11-14.11. 23.

692 13. V. Müller, F. Imkamp, E. Biegel, S. Schmidt and S. Dilling, *Ann. N. Y. Acad. Sci.*, 2008, **1125**, 137-
693 146.

694 14. P. L. Tremblay, T. Zhang, S. A. Dar, C. Leang and D. R. Lovley, *mBio*, 2012, **4**, e00406-00412.

695 15. J. Mock, Y. Zheng, A. P. Mueller, S. Ly, L. Tran, S. Segovia, S. Nagaraju, M. Köpke, P. Dürre and R.
696 K. Thauer, *J. Bacteriol.*, 2015, **197**, 2965-2980.

697 16. S. Wang, H. Huang, J. Kahnt, A. P. Mueller, M. Köpke and R. K. Thauer, *J. Bacteriol.*, 2013, **195**,
698 4373-4386.

699 17. S. Wang, H. Huang, J. Moll and R. K. Thauer, *J. Bacteriol.*, 2010, **192**, 5115-5123.

700 18. H. Latif, A. A. Zeidan, A. T. Nielsen and K. Zengler, *Curr. Opin. Biotechnol.*, 2014, **27**, 79-87.

701 19. M. Köpke, C. Held, S. Hujer, H. Liesegang, A. Wiezer, A. Wollherr, A. Ehrenreich, W. Liebl, G.
702 Gottschalk and P. Dürre, *Proc. Natl. Acad. Sci. USA*, 2010, **107**, 13087-13092.

703 20. C. Leang, T. Ueki, K. P. Nevin and D. R. Lovley, *Appl. Environ. Microbiol.*, 2012, **79**, 1102-1109.

704 21. R. Kerby and J. Zeikus, *Curr. Microbiol.*, 1983, **8**, 27-30.

705 22. M. Mohammadi, A. R. Mohamed, G. D. Najafpour, H. Younesi and M. H. Uzir,
706 *ScientificWorldJournal*, 2014, **2014**, Article ID 910590.

707 23. US7285402 B2, 2007.

708 24. B.-T. Xie, Z.-Y. Liu, L. Tian, F.-L. Li and X.-H. Chen, *Bioresour. Technol.*, 2015, **177**, 302-307.

709 25. Y. Tan, J. Liu, X. Chen, H. Zheng and F. Li, *Mol. Biosyst.*, 2013, **9**, 2775-2784.

710 26. H. Nagarajan, M. Sahin, J. Nogales, H. Latif, D. R. Lovley, A. Ebrahim and K. Zengler, *Microb. Cell.*
711 *Fact.*, 2013, **12**, 118.

712 27. E. Marcellin, J. B. Behrendorff, S. Nagaraju, S. DeTissera, S. Segovia, R. W. Palfreyman, J. Daniell,
713 C. Licona-Cassani, L.-e. Quek and R. Speight, *Green Chem.*, 2016, DOI: 10.1039/c5gc02708j.

714 28. J. M. Whitham, O. Tirado-Acevedo, M. S. Chinn, J. J. Pawlak and A. M. Grunden, *Appl. Environ.*
715 *Microbiol.*, 2015, **81**, 8379-8391.

716 29. Y. Tan, J. Liu, Z. Liu and F. Li, *J. Basic Microbiol.*, 2014, **54**, 996-1004.

717 30. M. Köpke, M. L. Gerth, D. J. Maddock, A. P. Mueller, F. Liew, S. D. Simpson and W. M. Patrick,
718 *Appl. Environ. Microbiol.*, 2014, **80**, 3394-3403.

719 31. H. L. Drake, A. S. Gossner and S. L. Daniel, *Ann. N. Y. Acad. Sci.*, 2008, **1125**, 100-128.

720 32. S. D. Brown, S. Nagaraju, S. Utturkar, S. De Tissera, S. Segovia, W. Mitchell, M. L. Land, A.
721 Dassanayake and M. Köpke, *Biotechnol. Biofuels.*, 2014, **7**, 40.

722 33. A. K. Jones, O. Lenz, A. Strack, T. Buhrke and B. Friedrich, *Biochemistry*, 2004, **43**, 13467-13477.

723 34. S. Watanabe, D. Sasaki, T. Tominaga and K. Miki, *Biol. Chem.*, 2012, **393**, 1089-1100.

724 35. S. Wang, H. Huang, J. Kahnt and R. K. Thauer, *J. Bacteriol.*, 2013, **195**, 1267-1275.

725 36. K. Schuchmann and V. Müller, *J. Biol. Chem.*, 2012, **287**, 31165-31171.

726 37. M. Köpke, C. Mihalcea, F. Liew, J. H. Tizard, M. S. Ali, J. J. Conolly, B. Al-Sinawi and S. D. Simpson,
727 *Appl. Environ. Microbiol.*, 2011, **77**, 5467-5475.

728 38. C. Vogel and E. M. Marcotte, *Nat. Rev. Genet.*, 2012, **13**, 227-232.

729 39. M. Rother, E. Oelgeschläger and W. W. Metcalf, *Arch. Microbiol.*, 2007, **188**, 463-472.

730 40. N. Matschiavelli, E. Oelgeschläger, B. Cocchiararo, J. Finke and M. Rother, *J. Bacteriol.*, 2012,
731 **194**, 5377-5387.

732 41. E. S. Arner and A. Holmgren, *Eur. J. Biochem.*, 2000, **267**, 6102-6109.

733 42. S. W. Ragsdale and L. G. Ljungdahl, *J. Bacteriol.*, 1984, **157**, 1-6.

734 43. J. Bertsch and V. Müller, *Biotechnol. Biofuels.*, 2015, **8**, 210.

735 44. E. Biegel, S. Schmidt, J. M. González and V. Müller, *Cell. Mol. Life Sci.*, 2011, **68**, 613-634.

736 45. W. Buckel and R. K. Thauer, *Biochim. Biophys. Acta*, 2013, **1827**, 94-113.

737 46. C. K. Lim, K. A. Hassan, S. G. Tetu, J. E. Loper and I. T. Paulsen, *PLoS One*, 2012, **7**, e39139.

738 47. D. Clarke and P. Bragg, *J. Bacteriol.*, 1985, **162**, 367-373.

739 48. F. Hillmann, R. J. Fischer and H. Bahl, *Arch. Microbiol.*, 2006, **185**, 270-276.

740 49. A. May, F. Hillmann, O. Riebe, R. J. Fischer and H. Bahl, *FEMS Microbiol. Lett.*, 2004, **238**, 249-
741 254.

742 50. S. Kawasaki, J. Ishikura, Y. Watamura and Y. Niimura, *FEBS Lett.*, 2004, **571**, 21-25.

743 51. S. Phadtare, J. Alsina and M. Inouye, *Curr. Opin. Microbiol.*, 1999, **2**, 175-180.

744 52. D. Amador-Noguez, I. A. Brasg, X. J. Feng, N. Roquet and J. D. Rabinowitz, *Appl. Environ.*
745 *Microbiol.*, 2011, **77**, 7984-7997.

746